Geochemistry Geophysics Geosystems G3

Article
Volume 14, Number 8
8 August 2013
doi: 10.1002/ggge.20175
ISSN: 1525-2027

Published by AGU and the Geochemical Society

Bimodal volcanism of the High Lava Plains and Northwestern Basin and Range of Oregon: Distribution and tectonic implications of age-progressive rhyolites

Mark T. Ford, Anita L. Grunder, and Robert A. Duncan

College of Earth, Ocean, and Atmospheric Sciences, Oregon State University, 104 CEOAS Administration Building, Corvallis, Oregon, 97331, USA (Fordm@geo.oregonstate.edu or MTF5512@yahoo.com)

[1] Multiple episodes of Oligocene and younger silicic volcanism are represented in the high lava plateau of central and southeastern Oregon. From 12 Ma to Recent, volcanism is strongly bimodal with nearly equal volumes of basalt and rhyolite. It is characterized by moderate to high silica (SiO_2 >72 wt. %) rhyolitic tuffs and domes that are younger to the west, and widespread, tholeiitic basalts that show no temporal pattern. We report 18 new $^{40}Ar/^{39}Ar$ incremental heating ages on rhyolites, and establish that the timing of the age-progressive rhyolites is decoupled from basaltic pulses. This work expands on that of previous workers by clearly linking the High Lava Plains (HLP) and northwestern-most Basin and Range (NWBR) rhyolite volcanism into a single age-progressive trend. The spatial-temporal relationship of the rhyolite outcrops and regional tectonics indicate that subsidence due to increasingly dense crust creates large, primarily sediment-filled basins within the more volcanically active HLP. The west-northwest age progression in rhyolitic volcanism is counter to the trend expected for a quasi-stationary mantle upwelling relative to North American plate motion. We attribute the rhyolitic age progression to mantle upwelling in response to slab rollback and steepening, and this is consistent with mantle anisotropy under the region and analog slab rollback models. This removes the necessity of deep mantle plume involvement. Laboratory experimental studies indicate that the geometry of the downgoing slab can focus upwelling or asthenospheric counterflow into a constricted band, resulting in greater volcanic volumes in the HLP as compared to the NWBR.

Components: 14,332 words, 7 figures, 2 tables.

Keywords: high lava plains; bimodal volcanism; intraplate volcanism; Ar-Ar geochronology; Oregon geology; slab rollback.

Index Terms: 1115 Radioisotope geochronology: Geochronology; 1033 Intra-plate processes: Geochemistry; 1031 Subduction zone processes: Geochemistry; 3613 Subduction zone processes: Mineralogy and Petrology; 3615 Intra-plate processes: Mineralogy and Petrology; 8170 Subduction zone processes: Tectonophysics; 3060 Subduction zone processes: Marine Geology and Geophysics; 8415 Intra-plate processes: Volcanology; 8413 Subduction zone processes: Volcanology.

Received 30 January 2013; **Revised** 6 May 2013; **Accepted** 14 May 2013; **Published** 8 August 2013.

Ford, M. T., A. L. Grunder, and R. A. Duncan (2013), Bimodal volcanism of the High Lava Plains and northwestern Basin and Range of Oregon: Distribution and tectonic implications of age-progressive rhyolites, *Geochem. Geophys. Geosyst., 14*, 2836–2857, doi:10.1002/ggge.20175.

1. Introduction

[2] The late Cenozoic tectonomagmatic evolution of the Pacific Northwestern United States is complex, involving three geodynamic mantle features: the Yellowstone hotspot, mantle processes related to the subduction of the Cascadia slab, and extension of the Basin and Range. These tectonic-magmatic elements contribute to the formation of the largest Cenozoic continental volcanic province in the world, including the Columbia River Basalts, Steens Basalts, volcanic provinces of the Yellowstone—Snake River Plain track, Owyhee Plateau and High Lava Plains (HLP), and northwestern-most Basin and Range (NWBR) (Figure 1) [*Smith and Luedke*, 1984; *Pierce and Morgan*, 1992; *Hooper et al*., 2002; *Shoemaker and Hart*, 2002]. This region is a modern example of intracontinental magmatic modification of the lithosphere.

[3] The HLP and NWBR physiographic provinces of Oregon (Figure 1) are prominent elements of this tectonically complicated region, and contain multiple episodes of Oligocene and younger volcanism. Over the past 12 Ma, silicic volcanism has produced a WNW age-progressive trend across the HLP-NWBR, nearly opposite from the trend of coeval age-progressive rhyolites of the Yellowstone-Snake River Plain system [*MacLeod et al*., 1976; *Jordan et al*., 2004]. In contrast, basaltic volcanism over the same period has not left a systematic temporal pattern in either the HLP-NWBR or Yellowstone-Snake River Plain provinces [cf., *Kuntz et al*., 1992; *Jordan et al*., 2004]. Most workers attribute the HLP age-progressive rhyolites to lithospheric processes such as extension [*Fitton et al*., 1991; *Christiansen et al*., 2002] or extension coupled with crustal block rotation [*Carlson and Hart*, 1987] or to a westward spread of a portion of the deep-seated Yellowstone plume head, with or without involvement of Cascadia slab subduction [*Draper*, 1991; *Camp and Ross*, 2004; *Jordan et al*., 2004]. Here we report 18 new $^{40}Ar/^{39}Ar$ age determinations for rhyolitic

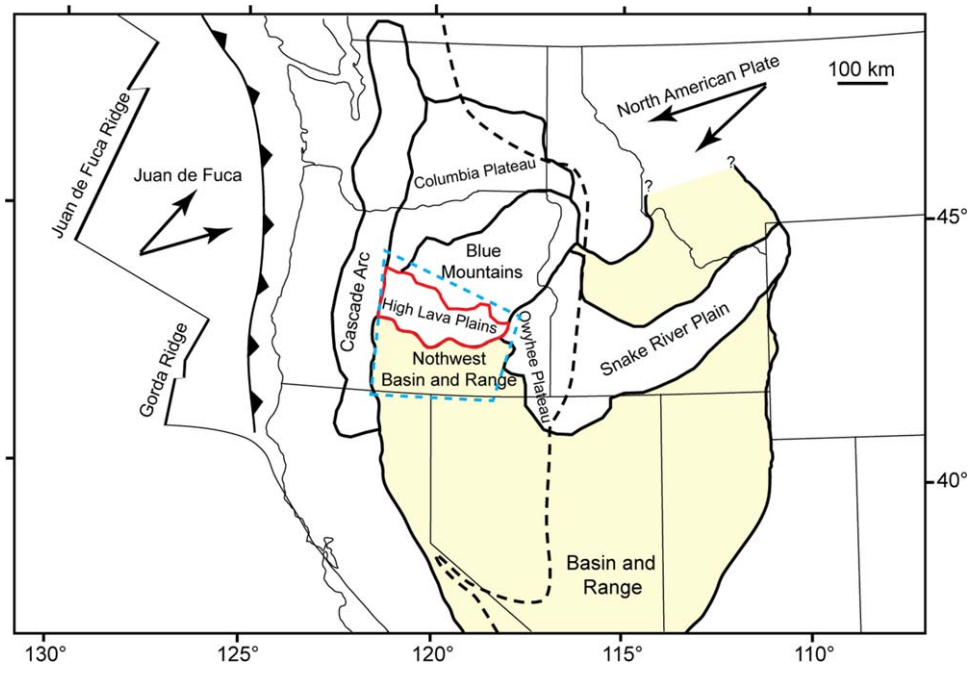

Figure 1. Regional tectonic setting of the High Lava Plains (outlined in red) and surrounding provinces. The Northwest Basin and Range refers to that portion of the Great Basin that extends into southern Oregon. Dashed line indicates approximate position of the $^{87}Sr/^{86}Sr$ 0.706 line [after *Kistler and Peterson*, 1978], representing the western edge of the Proterozoic or older craton of North America with generally Mesozoic and younger accreted terranes to the west. Lightly shaded region indicates middle Miocene and younger extensional normal faulting (Basin and Range style) [after *Pezzopane and Weldon*, 1993]. Two sets of arrows give the absolute plate motions and velocities based on the NUVEL-1A model of *DeMets, et al*. [1994] and the HS3-NUVEL-1A model of *Gripp and Gordon* [2002]. North American Plate motion is between 19 and 26 km/Ma in central Oregon, near the center of the studied area (outlined by blue dashed box) and the Juan de Fuca Plate ranges from 16 to 19 km/Ma. Physiographic provinces adapted after *Dicken* [1950]; *Walker and MacLeod* [1991]; *MacLeod, et al*. [1995]; *Shoemaker and Hart*, [2002].

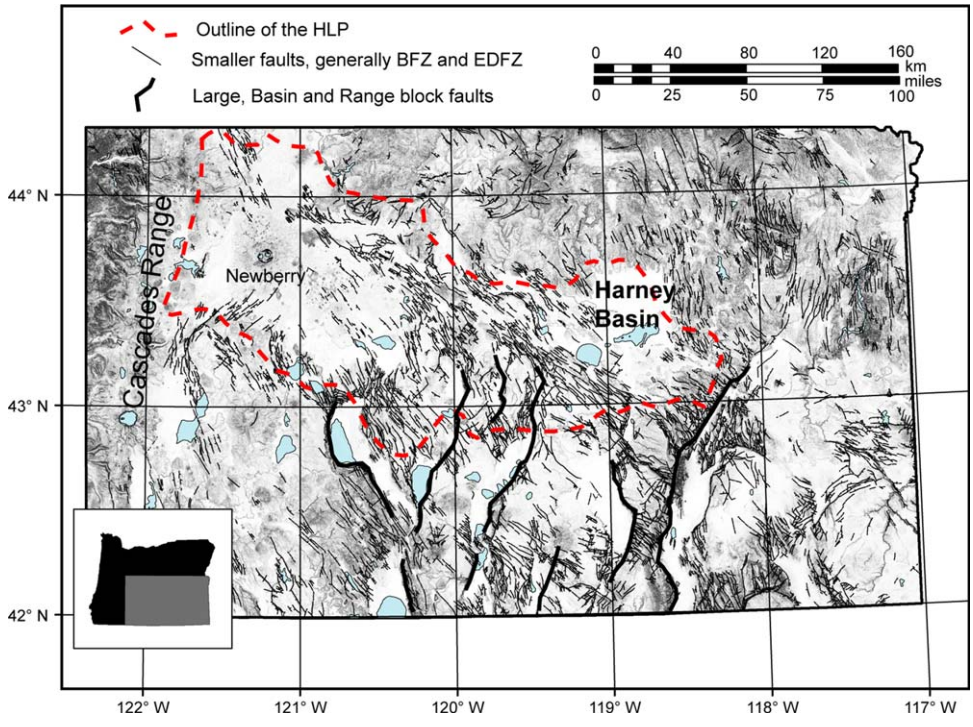

Figure 2. Slopeshade DEM and fault map of south-central and southeastern Oregon. Major, generally NNE trending Basin and Range type faults are shown with thick lines. Thin, generally NW trending lines obliquely cutting the HLP represent the Brothers Fault Zone while the NWBR is similarly cut but the Eugene—Denio Fault Zone. Heavy red dashed line outlines the HLP physiographic province as described in the text and Figure 1. The HLP has generally muted terrain (lighter shading) compared to surrounding provinces. Figure is adapted from the Oregon State Geologic Map [*Walker and MacLeod*, 1991] and simplified from the spatial database of *Miller et al*. [2003].

samples, mostly from the NWBR, and further document the distribution of westward age-progressive rhyolites within Oregon. We also provide a comprehensive, quantitative volume estimates for volcanic units in this bimodal province which has erupted nearly equal volumes of basalt-basaltic andesite and rhyolite over the past 12 Ma. Cascadia slab plate-driven asthenospheric flow is the driving force of our model for volcanism in the HLP and NWBR and no plume is required.

1.1. Physiographic and Tectonic Background of the HLP-NWBR

[4] Since the original reconnaissance mapping surveys of *Russell* [1884, 1905], there has been persistent interest in the igneous rocks and tectonics of the HLP-NWBR region [e.g., *Williams*, 1935; *Green*, 1973; *Wells*, 1979; *Carlson and Hart*, 1987; *Draper*, 1991; *Johnson and Ciancanelli*, 1984; *Johnson and Grunder*, 2000; *Jordan et al*., 2004; *Boschmann*, 2012]. Much of the work over the past three decades is contained in university student theses with a few specific areas receiving concentrated study (e.g., Glass Buttes). The recent geophysical and geological investigation of the HLP has sparked a comprehensive body of work, much of which is distilled in this Geochemistry Geophysics Geosystems volume.

[5] The physiographic HLP (Figure 1) generally comprises a late Miocene and younger volcanic province that is approximately 90 km wide and 275 km long extending across eastern and central Oregon. It is bounded by the Owyhee Plateau, Cascades volcanic arc, extending Basin and Range (the NWBR) and to the north by the relatively unextended, accreted terranes of the Blue Mountains region. Generally, late Miocene and younger flat-lying basaltic lava flows, ignimbrites and volcaniclastic sediments cover much of the muted topography that characterizes the HLP (Figure 2). Oligocene through middle Miocene silicic volcanic rocks are also sparsely exposed within the HLP [*MacLeod et al*., 1976; *McKee and Walker*, 1976; *Jordan et al*., 2004] (Figures 3a and 3b).

[6] The HLP is cut obliquely by the Brothers Fault Zone, which is characterized by small, northwest-

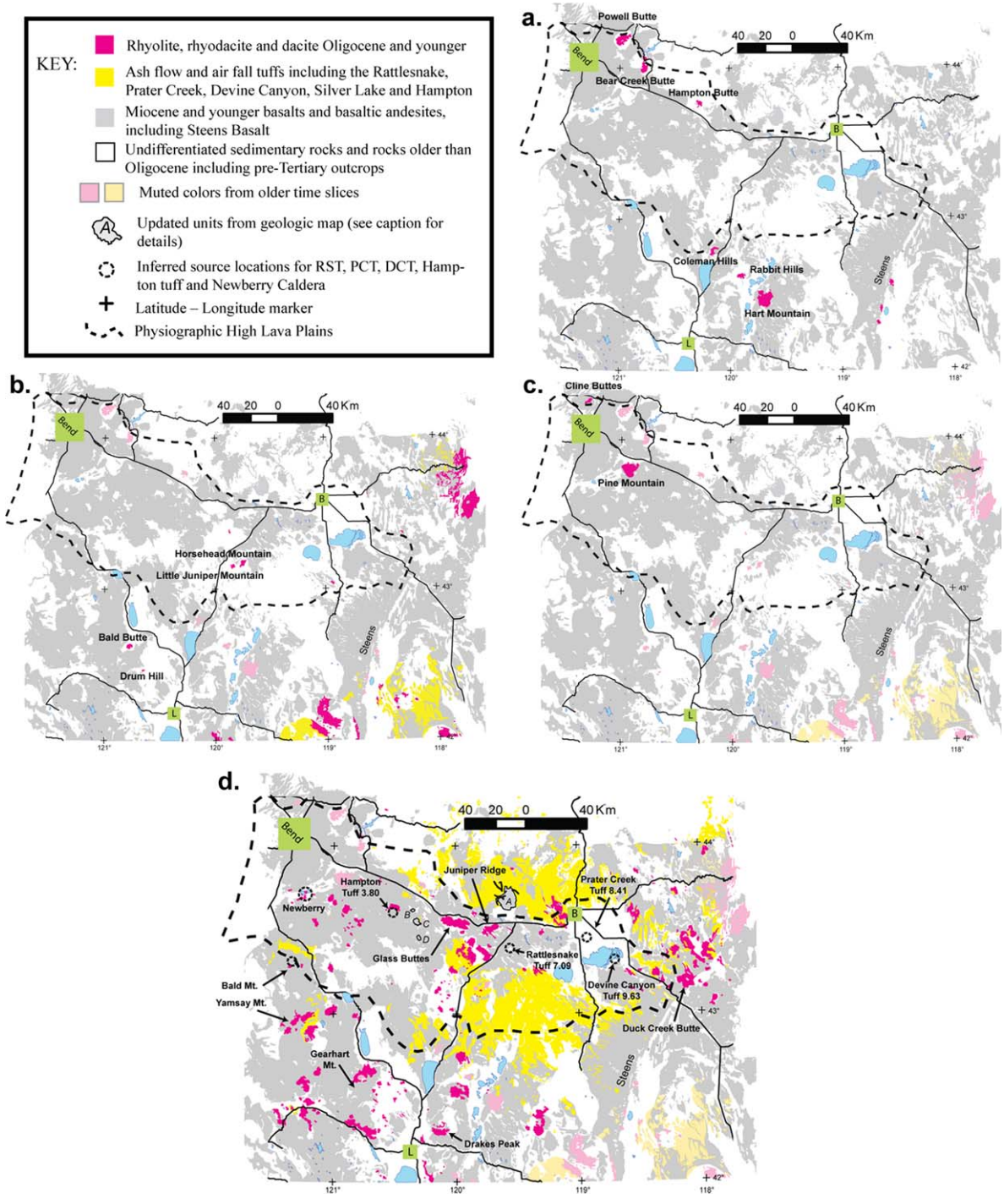

Figure 3. Map of the distribution of central and eastern Oregon rhyolites and basalts shows the spatial distribution of silicic lavas and tuffs though time with (a) John Day age (37–20 Ma), (b) Steens age (~17.5–15 Ma), (c) Deschutes age (7–6 Ma), and (d) age-progressive HLP and NWBR <12 Ma province. Lettered, outlined, areas on Figure 3d indicate units that differ from the *Walker and MacLeod* [1991] Oregon State geologic map as follows: (*A*) basalt of Dry Mountain (originally mapped as an andesite, *Iademarco* [2009]), (*B*) basalt or basaltic andesite with local hydrothermal silica sinter, (*C*) basalt or basaltic andesite, (*D*) basalt or basaltic andesite. Units *B*, *C*, and *D* were originally mapped as rhyolite. HLP volcanic province extends east of the physiographic HLP and includes Duck Creek Butte (Duck Butte Eruptive Center) and Jordan Craters. Proposed location for the Rattlesnake Tuff source [*Streck and Grunder*, 1997] given and proposed locations of vents, based in part from this map and field evidence (Grunder, unpublished) for other tuffs (Hampton, Prater Creek and Devine Canyon) shown with dashed circles. Black lines are major roads; heavy black dashed line outlines the HLP physiographic province from Figure 1. Green boxes are locations of major towns including Bend, Burns, and Lakeview. Many of the locations mentioned in the text are given and all four maps cover the same region.

Table 1. New $^{40}Ar/^{39}Ar$ Age Determinations (in Ma) From This Study[a]

Sample Number	Local Name	Age Type[b]	wt% K_2O if WR	Accepted (Plateau) Age	2σ Error	2σ percent	% Radio-Genic Ar 40	Inverse Isochron Age	2σ Error
MTF 07-04	Glass Buttes "A"	WR	4.20	5.79	0.04	0.75	98.49	5.74	0.11
MTF 07-05	Glass Buttes "E"	WR	4.48	6.49	0.05	0.80	100	6.49	0.06
MTF 07–38	North Connelly Hills	WR	3.72	5.59	0.05	0.86	77.7	5.59	0.07
MTF 07–16	Cougar Mt (Lake Co.)	WR	3.82	4.34	0.05	1.08	99.59	3.92	0.58
MTF 07–10	Devine Canyon Tuff	san		9.63	0.05	0.55	94.93	9.61	0.06
KCS 06-06	Alkali Buttes	san		7.26	0.05	0.66	100	7.25	0.05
MTF 07–49	Bug Butte (top)	plag		5.17	0.09	1.65	98.57	5.10	0.10
MTF 07–37	Spodue Mt (top)	plag		5.77	0.07	1.19	100	5.81	0.12
MTF 07–58	Drake Peak (Trf)	plag		8.96	0.06	0.64	95.84	8.95	0.13
MTF 07–52	Quartz Mountain Pass	bt		6.79	0.04	0.58	80.32	6.81	0.08
MTF 07–30	Cougar Peak (top)	plag		6.87	0.07	1.06	55.55	6.94	0.08
MTF 07–29	Dome south of Cox Flat	san		8.05	0.04	0.52	99.84	8.07	0.06
MTF 07–14	Hagar Mountain (top)	plag		5.67	0.16	2.83	100	5.73	0.28
MTF 07–53	Fergason Mountain	plag		6.16	0.04	0.62	99.66	6.16	0.06
MTF 07–34	Bald Butte	san		17.53	0.08	0.45	97.12	17.54	0.10
MTF 07–26	Drum Hill	plag		17.30	0.09	0.53	98.71	17.33	0.11
MTF 07–57	Twenty Mile Creek	san		15.03	0.08	0.56	100	15.04	0.09
MTF 07-02	Pine Mountain	WR	2.75	6.25	0.03	0.52	43.67	6.25	0.04

[a]In all cases, the plateau age and inverse isochron age are within 2σ of each other and the plateau age is preferred. See Figure 4 for age spectra from each sample and Table S1 for sample location.

[b]WR = whole rock minicore, san = sanidine mineral separate, bt = biotite mineral separate, plag = plagioclase series mineral separates with whole rock K_2O values given.

striking normal faults with offsets generally <10 m [*Lawrence*, 1976] (Figure 2). Large range-bounding normal faults of the Basin and Range gradually decrease in topographic and structural offset northward into the HLP (Figure 2). Although subtle, we use this preexisting, long-standing physiographic division to separate igneous rocks of the HLP from those of the NWBR. While we use the physiographic boundaries for the HLP in figures, the HLP volcanic province extends further east to include the Duck Butte Eruptive Center and Jordan Craters.

[7] The NWBR (Figure 1) is that part of the Great Basin within Oregon, occurring between Steens Mountain and the Cascade Arc, south of the HLP. The NWBR is cut by middle Miocene and younger Basin and Range style block faults [*Pezzopane and Weldon*, 1993] with scarps as high as 2000 m (e.g., Steens Mountain, Abert Rim). There are also diffuse northwest-striking faults, similar to the Brothers Fault Zone faults, comprising the less documented Eugene-Denio Fault Zone (Figure 2). Some vent complexes (e.g., Four Craters, Buttes of the Gods) mimic the regional NW to WNW fabric of these low-relief faults but there are not any vent alignments that parallel the larger offset, generally NNE striking "Basin and Range" faults. Compared to the HLP there are more exposures of the older (>12 Ma) silicic volcanic rocks in the NWBR due to the greater structural relief [cf., *Scarberry*, 2007] (Figures 3a and 3b), some of which were dated in this work (Table 1).

1.2. Geochronology and Geologic Background of the HLP-NWBR

[8] The volcanic rocks younger than 12 Ma in the HLP and NWBR make up a basalt-rhyolite bimodal province that consists of widespread, thin basalt lava flows and rhyolitic domes, lava flows and ash-flow tuffs, intercalated with tuffaceous sediments. The basalts are dominantly low-K high-alumina olivine tholeiites, with the most primitive resembling mid-ocean ridge basalts [*Hart et al*., 1984]. The basalts do not exhibit any age-progressive behavior, in contrast to the rhyolites, but do seem to focus in time to the axis of the HLP [*Jordan et al*., 2004]. Basalt eruptive activity was concentrated in up to four pulses, with the largest regional pulse around 7.5–8 Ma, and the most recent pulse of ~50,000 years located at either end of the HLP volcanic province, at Diamond and Jordan Craters and around Newberry Volcano.

[9] Rhyolites of the HLP-NWBR volcanic province erupted in an age-progressive manner, beginning in the east at around 10–12 Ma and younging to the west-northwest, with the youngest eruptions (<1 Ma) near Newberry Volcano. We exclude Newberry Volcano (<0.6 Ma) from the HLP as it has previously been associated with Cascades

volcanism [*Donnelly-Nolan et al*., 2008; *Jensen et al*., 2009; *Graham et al*., 2009]. This west-northwest-younging age progression has posed a tectonic puzzle in that it propagates in the opposite direction to the age progression of the rhyolites that define the Yellowstone-Snake River Plain trend [*Pierce and Morgan*, 1992], and nearly perpendicular to North American plate motion. *Jordan et al*. [2004], who link the two parallel age-progressive trends of the HLP and NWBR to form a single province, term the entire suite the "HLP trend", which we prefer, in contrast to *Humphreys et al*. [2000] and *Xue and Allen* [2006] who refer to the trend as the "Newberry hotspot" and "Newberry trend" respectively.

[10] More than 60 rhyolitic dome complexes dot the region (Figure 3). While some are clearly monogenetic, many are larger, more complex, polygenetic dome complexes like Glass Buttes or Juniper Ridge. They are elongate in a northwesterly direction, parallel to the grain of the Brothers Fault Zone, and have internal age trends that young to the west. Many of these domes are dated in this work (Table 1) and many more were dated by *Jordan et al*. [2004] or reported in *Fiebelkorn et al*. [1983]. Table S1 (supporting information)[1] contains a summary of ages from silicic rocks of the HLP-NWBR.

[11] Three large 100–300 km^3 dense rock equivalent (DRE) ash-flow tuffs had sources in the Harney Basin and crop out extensively (Figure 3d) including the Devine Canyon Tuff (DCT), Prater Creek Tuff (PCT), and Rattlesnake Tuff (RST). Only the RST has been studied in detail [e.g., *Streck*, 2002; *Streck and Grunder*, 1995, 1997, 1999, 2008, 2012]. A few of the domes have vented smaller volume ash-flow tuffs that are still preserved and there are likely more, yet undocumented, small volume $<$12 Ma tuffs in the HLP and NWBR.

[12] There are three major episodes of Cenozoic volcanic activity in the region that predate volcanism of the HLP-NWBR. The Clarno Formation (54–40 Ma) crops out to the north and west of the HLP in the Blue Mountains Terrane (Figure 1) to thicknesses $>$1800 m [*Walker and Robinson*, 1990; *Bestland and Retallack*, 1994a] and likely underlies the HLP. The John Day Formation (38.5–20 Ma) crops out to thicknesses $>$1000 m, primarily to the north of the HLP-NWBR [*Robinson et al*., 1990; *Bestland and Retallack*, 1994b] but also within the HLP-NWBR (Figure 3a). Along the northern margin of the HLP volcanism at Hampton Butte [*Iademarco*, 2009], Bear Creek Butte and Powell Buttes [*Evans and Brown*, 1981] are similar in age and composition, and they have been ascribed to the John Day Formation. Somewhat younger volcanism from 22 to 20 Ma is exposed along faults in the NWBR. This includes the Coleman Hills [*Scarberry et al*., 2010], Rabbit Hills [Scarberry, 2007], and Hart Mountain [*Mathis*, 1993] which are similar in composition but not yet assigned to the John Day Formation.

[13] The Steens Basalt lava flows, with a volume up to 60,000 km^3 extend over the eastern part of the study area and into Idaho, Nevada and California [*Carlson and Hart*, 1987], and are contemporaneous with regional silicic eruptions from 17.5 to 15 Ma [*Brueseke et al*., 2008; *Coble and Mahood* 2012]. Isolated silicic domes 17.5–15.3 Ma are exposed as kipukas both within the HLP (e.g., Horsehead Mountain, Little Juniper Mountain, and Jackass Butte, *Jordan et al*. [2004]) and NWBR (e.g., Drum Hill and Bald Butte, Table 1; Figure 3b). The early to middle Miocene Strawberry Volcanic Field and various ash-flow tuffs (e.g., Sucker Creek, Littlefield, Dinner Creek: *Walker and MacLeod* [1991]) crop out northeast of the HLP (Figure 3b).

[14] Finally, we do not include rocks of the Deschutes Formation (7.4–4.0 Ma) which lies primarily north of Bend and consist predominantly of pyroclastic flow deposits and volcaniclastic sediments shed from the High Cascades [*Smith et al*., 1987; *Eungard*, 2012]. The Deschutes Formation also contains isolated 7–6 Ma domes including the Steelhead Falls rhyodacite and Cline Buttes rhyolite [*Sherrod et al*., 2004] (Figure 3c), which are associated with High Cascades Arc volcanic activity [*Taylor*, 1981]. We also exclude Newberry Volcano from the HLP volcanic province.

2. Methods

[15] Some samples were selected from undated silicic centers to better characterize the age progression of the HLP-NWBR while other samples were chosen for analysis to reduce the uncertainly or confirm the accuracy of previous K-Ar dates. Generally, new ^{40}Ar/^{39}Ar dates have at least an order of magnitude better precision compared with previously reported K-Ar dates. Additionally,

[1]Additional supporting information may be found in the online version of this article.

samples with very high Rb/Sr ratios were preferentially targeted so that with the more accurate ages, we could achieve more accurate initial radiogenic isotopic values [cf., *Ford*, 2012]. Samples for this work are a subset of samples selected for regional geochemical analyses [cf., *Ford*, 2012].

[16] Ages for nineteen rhyolitic samples, primarily from the NWBR, were determined by the $^{40}Ar/^{39}Ar$ incremental heating method at the Noble Gas Mass Spectrometry Laboratory at Oregon State University. Samples were prepared as either mineral separates (e.g., plagioclase, sanidine, biotite) or whole rock minicores. Cores were prepared from fresh, nonhydrated obsidian or from unaltered, homogeneous, devitrified whole rock. Argon extraction and analysis, using either a Heine low-blank, double-vacuum resistance furnace (whole rock cores, $n = 5$) or a Merchantek integrated 10W CO_2 continuous fire laser (mineral separates, $n = 14$), followed the methods described by *Duncan and Hogan* [1994], *Duncan et al*. [1997], and *Duncan and Keller* [2004] using a Fish Canyon Tuff biotite (FCT-3) monitor age of 28.02 ± 0.16 Ma [*Renne et al*., 1998]. Irradiation was at the Oregon State University 1 MW TRIGA experimental reactor facility. The neutron flux was calculated from analyses of the FCT-3 standard. The total decay constant (λ_{tot}) incorporating the $^{40}K_{(ec,p)}{}^{40}Ar$ and $^{40}K_{(B-,n)}{}^{40}Ca$ decays was 5.543×10^{-10} yr^{-1} as suggested by *Steiger and Jager* [1977]. Data reduction was done with the ArArCALC v2.2 software package [*Koppers*, 2002]. External errors (2σ) incorporate errors on decay constants, analytical errors (regressions on peak heights versus time) and errors in fitting measurements of monitors (J values), as suggested by *Koppers* [2002] and *Min et al*. [2000].

[17] We use the plateau age preferentially over the isochron age in all cases because age uncertainty is lower, resulting from generally low dispersion of step compositions in isochron plots. We define a plateau as five concordant, sequential steps comprising at least 50% of the total argon released. Concordant plateau and isochron ages indicate a trapped argon component (initial composition) that is within error of atmospheric composition.

3. Results

3.1. Age Determinations

[18] Of the 19 samples dated, 17 yielded $^{40}Ar/^{39}Ar$ age spectra plateaus concordant with sample isochron ages (within 2σ) (Table 1). One sample from Pine Mountain yielded a six-step plateau concordant to the isochron age but with only 44% of the ^{39}Ar released, and one sample from Dead Indian Mountain failed to produce a reliable crystallization age. Age spectrum plots are shown in Figure 4. Error (external) is reported to 2σ for all analyses, and in nearly all cases, errors are <2% of the calculated age and often <1%. Some ages of previously dated units changed significantly. For example, the age of the Drake Peak rhyolite has been updated from 14.7 ± 2 Ma [*Wells*, 1979; *Fiebelkorn, et al*., 1983] to 8.96 ± 0.06 Ma and the age of Quartz Mountain from 7.8 ± 0.4 Ma [*Fiebelkorn, et al*., 1983] to 6.79 ± 0.04 Ma (Table 1). In all cases, precision was improved over previous K-Ar dates, sometimes significantly as exemplified at the Connelly Hills with a K-Ar date of 6.35 ± 0.65 Ma [*Fiebelkorn, et al*., 1983] compared to our $^{40}Ar/^{39}Ar$ date of 5.59 ± 0.05 Ma (Table 1). Our result for the DCT is very similar to those previously reported using $^{40}Ar/^{39}Ar$ total fusion analyses of single crystals. We report an age of 9.63 ± 0.05 Ma based on a 10-step heating plateau (Figure 4) recovering 94.9% of the radiogenic argon which is only slightly less than the weighted mean total fusion date of 9.74 ± 0.04 Ma returned using 9–10 single-grain analyses [*Jordan et al*., 2004]. Three obsidian whole rock minicores were analyzed, viz: Glass Buttes "A" (5.79 ± 0.04 Ma), Glass Buttes "E" (6.49 ± 0.05 Ma) and Cougar Mountain (4.34 ± 0.05 Ma) (Table 1). These samples released the majority of their ^{39}Ar during one heating step, generally between 1075°C and 1250°C, even using heating steps as small as 25°C (Figure 4).

[19] The vast majority of the new ages from this study fall within the 12–0 Ma range which largely confirm earlier work. We also report some new ages that do not fit the 12–0 Ma westward age sweep of the HLP-NWBR volcanic province. We identify previously unknown middle Miocene volcanic centers at Bald Butte (17.53 ± 0.08 Ma) and Drum Hill (17.30 ± 0.09 Ma) (Figure 3b and Table 1). We report a new age of 6.25 ± 0.03 Ma (Table 1) for rhyolite located at the top of Pine Mountain, and we believe this to be a reliable crystallization age despite the plateau containing only 44% of the total Ar released.

3.2. Erupted Volumes

[20] While some estimates of the volumes of specific units or flows in the HLP have been calculated [e.g., *Streck and Grunder*, 1995], there has been no comprehensive reporting of the volcanic volumes

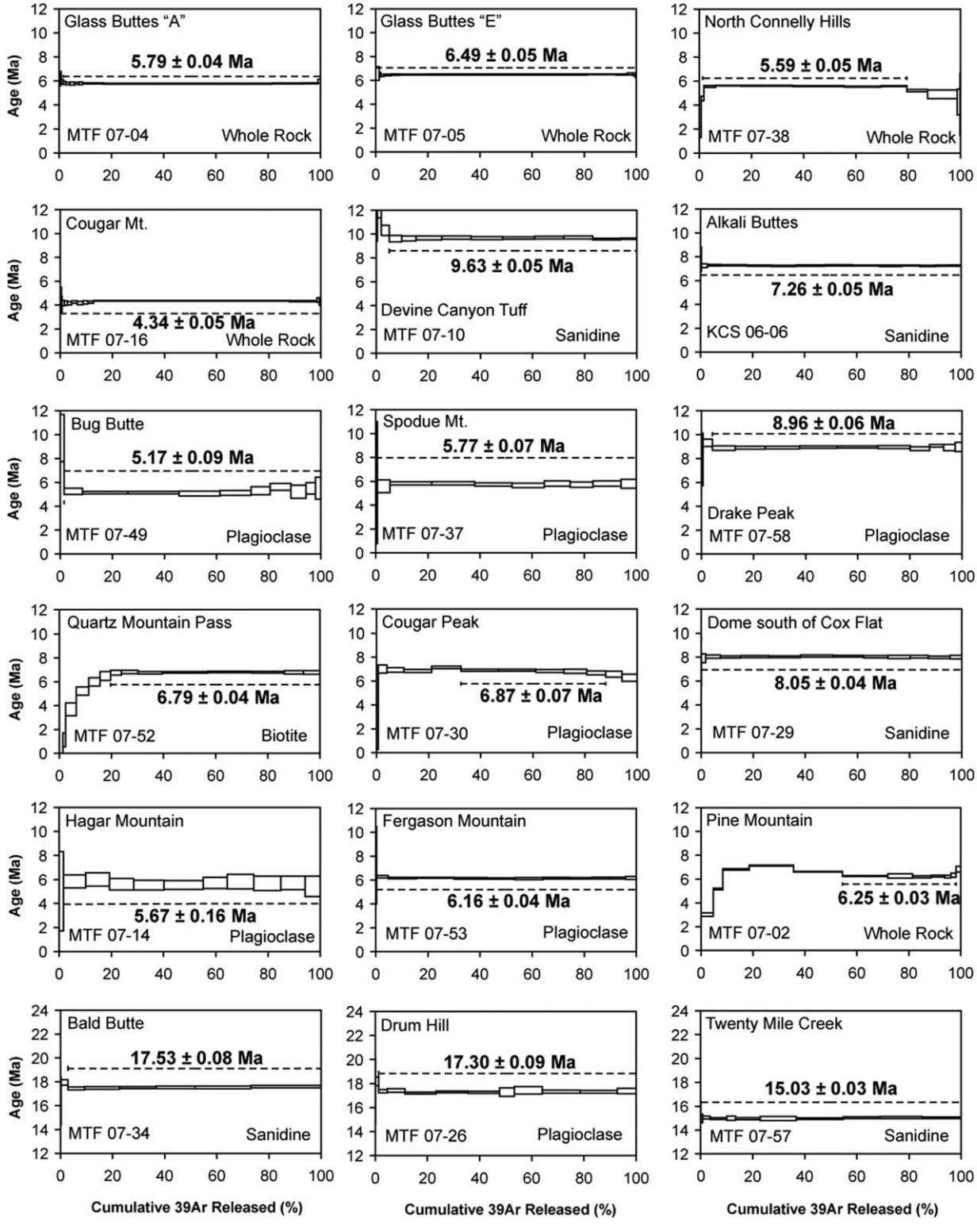

Figure 4. New age determinations for the HLP and NWBR. Eighteen $^{40}Ar/^{39}Ar$ age plateaus from the current study, 15 of which are from <12 Ma samples from the NWBR or HLP with one of these (Pine Mountain, 6.25 Ma) ascribed to the Deschutes Formation (see text and Table 1). The remaining three samples fall within the "Steens-age" time slice from 18 to 15 Ma (Figure 3b). Dashed lines on the diagrams indicate the heating steps that were integrated into the age calculation, the width of each box is the percent of total ^{39}Ar released for that temperature step, and the height of each box is the 2σ uncertainty for that heating step.

Table 2. Estimated <12 Ma Volcanic Volumes Within the HLP and NWBR[a]

Location	Minimum (km^3)	Maximum (km^3)
Deschutes formation	negligible	100
This study, 12–0 Ma HLP and NWBR	2000	2500
Newberry related, including basalts	800	1000
Total	2800	3600

[a]Additional volumes of the Deschutes and some Newberry related flows extend outside the physiographic HLP and NWBR and are not included here. Total eruptive volumes considered for this study (see text) are 1000–1250 km^3 of basaltic, 1000–1250 km^3 of rhyolitic, and ~100 km^3 of intermediate composition volcanic rocks.

for the <12 Ma HLP-NWBR system. Our total volume estimate for volcanism <12 Ma in the study area is 2000–2500 km^3 (Table 2) which contains subequal volumes of basalt and rhyolite and a minor amount of intermediate compositions. Although basalts, rhyolite domes and tuffs are widely exposed (Figure 3), estimating the thickness and thus total volume of these 12–0 Ma volcanic products is difficult. Cross sections through the volcanic units are exposed only in substantial fault scarps, mainly in the NWBR, and in a few rare canyons in the HLP. Logs from a few energy exploration drill holes indicate that intercalated sediments and "Miocene and younger" undifferentiated volcanic rocks extend to depths of >1.5 km within the Harney Basin in the HLP [*Milliard*, 2010] and >3.5 km west of Lakeview in the NWBR [*Popenoe*, 1961; *Newton et al*., 1962]. Recent geophysical studies [*Cox*, 2011] indicate that Cenozoic intercalated sediments and volcanic rocks may be >7 km thick in the eastern Harney Basin, which is likely the locus of calderas for the Devine Canyon and PCTs. Field work and previous studies (see later) have indicated that the 12–0 Ma volcanic rocks generally make up only a thin veneer where exposed, and while the Harney Basin may have appreciable volumes of these younger rocks, we consider it more likely that the basin contains mostly sediments and volcaniclastic rocks with only a limited volume of <12 Ma basalts and rhyolites.

3.2.1. Rhyolite Volume

[21] We estimate the total volume of <12 Ma rhyolitic volcanism in the study area is 1000–1250 km^3, the majority of which is represented by the three major ash-flow tuffs in the HLP. *Streck and Grunder* [1995] calculated the volume of the RST at 280 km^3 DRE. The PCT and DCT (Figure 3) are estimated to be 100–150 and 200–300 km^3 respectively [*Green*, 1973]. We chose the higher end of Green's estimate for the DCT as its extent and thickness are at least as great as those for the RST. Large tuffs (over 100 km^3) do not occur in the NWBR or western HLP and all large tuffs are older than 7 Ma.

[22] The smaller tuffs of the region are <40 km^3 each and as small as 1 km^3 and source areas are often inferred based on location and age (reference Figure 3 for many of the following locations and Table 1 or Table S1 for additional ages). Frederick Butte is the likely source of the Tuff of Espeland Draw [*Fiebelkorn, et al*., 1983; *Walker*, 1974; *Johnson*, 1998], which has been correlated with the Hampton Tuff ($^{40}Ar/^{39}Ar$ age of 3.80 ± 0.16 Ma) by *Iademarco* [2009]. The maximum volume of the Hampton Tuff is estimated to be 40 km^3 [*Tucker et al*., 2011]. A number of smaller tuffs have unidentified sources. The Peyerl Tuff, located on the margins of and within maars of the Fort Rock Basin, may be associated with an inferred caldera structure at Wart Peak and Bald Mountain [*Fiebelkorn, et al*., 1983; *MacLeod, et al*., 1976]. We estimate the volume to be between 5 and 20 km^3 (DRE). The peralkaline tuff of Wagontire Mountain, mapped by *Walker and Swanson* [1968], has an approximate volume of 1 km^3 (DRE) and a postulated source just west of Wagontire Mountain but it has not been dated. The Buckaroo Lake Tuff has a $^{40}Ar/^{39}Ar$ age of 6.85 ± 0.04 Ma, overlapping within error of nearby Elk Mountain [*Jordan et al*., 2004] but no source has been identified. The Silver Creek Welded Tuff may be sourced in the Yamsay Mountain area [*Hering*, 1981] but *MacLeod et al*. [1976] disagreed based on a K-Ar age of 6.77 ± 1.10 Ma, which is older than other domes in the area. We estimate the volume of this tuff to be between 5 and 20 km^3 (DRE), assuming a Yamsay Mountain source. The Plush Tuff, exposed at Hart Mountain, is undated and has a possible source near Beatys Butte [*Mathis*, 1993; *Larson*, 1965]. The volume estimate of the smaller tuffs is based on outcrop coverage and thickness from previous reconnaissance mapping and by using the approximations of *Streck and Grunder* [1995] to account for erosional loss, air fall, and conversion to DRE, using the RST as an analog. The total volume of all of the tuffs is likely 800–850 km^3.

[23] To the rhyolite volume of the tuffs, we added 150–400 km^3 from the silicic domes, many of which are <1 km^3, and their associated ash fall deposits. Some of the larger complexes may be as much as 50 km^3. The 6.5–5.7 Ma Glass Buttes complex (Figure 3) is 20 km long, 2–5 km wide and while variable in thickness, rhyolite extends to depths of at least 1 km in places, based on

hydrothermal energy exploration drilling [*Johnson and Ciancanelli*, 1984]. This yields a volume estimate of approximately 25–50 km^3 for the complex. The silicic rocks of Drake Peak (Figure 3), located in the NWBR, are likewise estimated to have a volume of 25–50 km^3 (based on cross sections of *Wells* [1979]). Other centers are intermediate in size, including the Duck Butte Eruptive Center, which is estimated to be 7 km^3 [*Johnson and Grunder*, 2000] and Juniper Ridge (Figure 3), which is conservatively estimated to be 3 km^3 [*Maclean*, 1994]. The total volume of silicic domes and flows is estimated to be 120–250 km^3.

[24] The main sources of error in the volume estimate of the rhyolites are uncertainties in thickness and the unknown quantity of dispersed pyroclastic fall deposits. Two very recent, local analogs provide insight in to the amount of pyroclastic fall deposits that these eruptions might have produced. The 700 C.E. eruption of the Big Obsidian Flow at Newberry Volcano (Figure 3) has a well documented associated plinian fall deposit of 0.1 km^3 (DRE), or about 40% of the total eruption [*Jensen*, 2006]. Both the 950 C.E. and 1100 C.E. Little Glass Mountain and Glass Mountain flows of the Medicine Lake Volcano yielded about 10% by volume (DRE) of tephra [*Heiken et al*., 1978; *Donnelly-Nolan et al*., 1990]. Using these eruptions as proxies for HLP-NWBR volcanism would add an estimated 12–100 km^3 to the volume of the silicic domes in the region.

3.2.2. Basalt and Intermediate Composition Volume

[25] Most of the <12 Ma basalts and basaltic andesites in the HLP and NWBR are low-K, high-alumina olivine tholeiites but subordinate calc-alkaline and alkali basalts exist [cf., *Hart et al*., 1984; *Jordan*, 2002; *Streck and Grunder*, 2012]. Areal coverage is estimated to be ~25,000 km^2, roughly 1/2 of the study area, with a greater concentration of flows along the axis of the HLP and few exposures east of 119.5° in the NWBR. High-alumina olivine tholeiite flows are commonly 5 to 30 m thick [*Hart et al*., 1984; *Mathis*, 1993; *Johnson*, 1995; *Scarberry*, 2007; *Iademarco*, 2009] where normal faults or canyons expose cross sections of basalt. Individual flow fields commonly occur as compound stacks of several to a dozen flows with no evidence of erosion or soil development between stacks. Multiple stacks of flows, separated by tuffaceous sediments or volcanic rocks, are exposed for ~100 m at Hampton Buttes [*Iademarco*, 2009], in drill core for ~40 m at Glass Buttes [*Johnson*, 1984], for ~55 m at Abert Rim [*Scarberry et al*., 2010] and for ~50 m at Burma Rim [*Jordan et al*., 2002]. Three distinct stacks of flows, ranging in age from 7.9 to 4.0 Ma [*Jordan et al*., 2004], each with distinctive flow thicknesses and morphologies, crop out in Dry River Canyon (HLP). These three flow stacks are separated by unconformities and make a composite thickness of ~100 m, representing one of the few thick exposures of mafic lavas in the HLP. Multiple different models, some of which factor the greater aerial coverage and greater thickness along the axis of the HLP and less coverage and thickness across the NWBR, converge to yield a total volume of basaltic and basaltic andesite volcanic rocks of 1000–1250 km^3, roughly equivalent to that of the rhyolites.

[26] The majority of the volume of intermediate compositions (andesites and dacites) is associated with Gearhart Mountain in the NWBR (Figure 3). Gearhart Mountain has a composite shield morphology and is primarily andesite, with subordinate volumes of basalts, dacites and rhyolites [*Brikowski*, 1983]. Yamsay Mountain (Figure 3), also in the NWBR, contains a number of intermediate composition samples in the literature, but the bulk of the estimated 150 km^3 shield volcano is basaltic andesite [*Hering*, 1981]. Hagar Mountain, again in the NWBR, has an unknown volume of intermediate rocks but a total volcanic volume likely <20 km^3. Intermediate compositions in the HLP [cf., *Maclean*, 1994; *Johnson*, 1995] are over sampled with respect to their volume and total volumes are not great, likely <20 km^3 in total. Thus, the total volume of intermediate rocks (andesite and dacite) from the HLP and NWBR is approximately 100 km^3, about 5% of the total volume of volcanic rocks of for the <12 Ma time period.

3.2.3. Localized Events Excluded in This Volume Estimate

[27] We do not include Newberry Volcano in our volume estimate of the <12 Ma HLP-NWBR and this shield has a volume of 800–1000 km^3 [*MacLeod et al*., 1995]. We also exclude the Deschutes Formation and Pine Mountain which falls within the 12–0 Ma age range and crops out it the northwest portion of the physiographic HLP. We limit the volume related to the Deschutes Formation in the HLP to ~100 km^3 (Table 2).

3.3. Geologic Map Updates

[28] In Figure 3d, we provide some minor updates to the state geologic map [*Walker and MacLeod*, 1991] that were discovered during field work. These include the basalt of Dry Mountain [*Iademarco*, 2009] and three nearly circular, flattened dome-like formations which from a distance

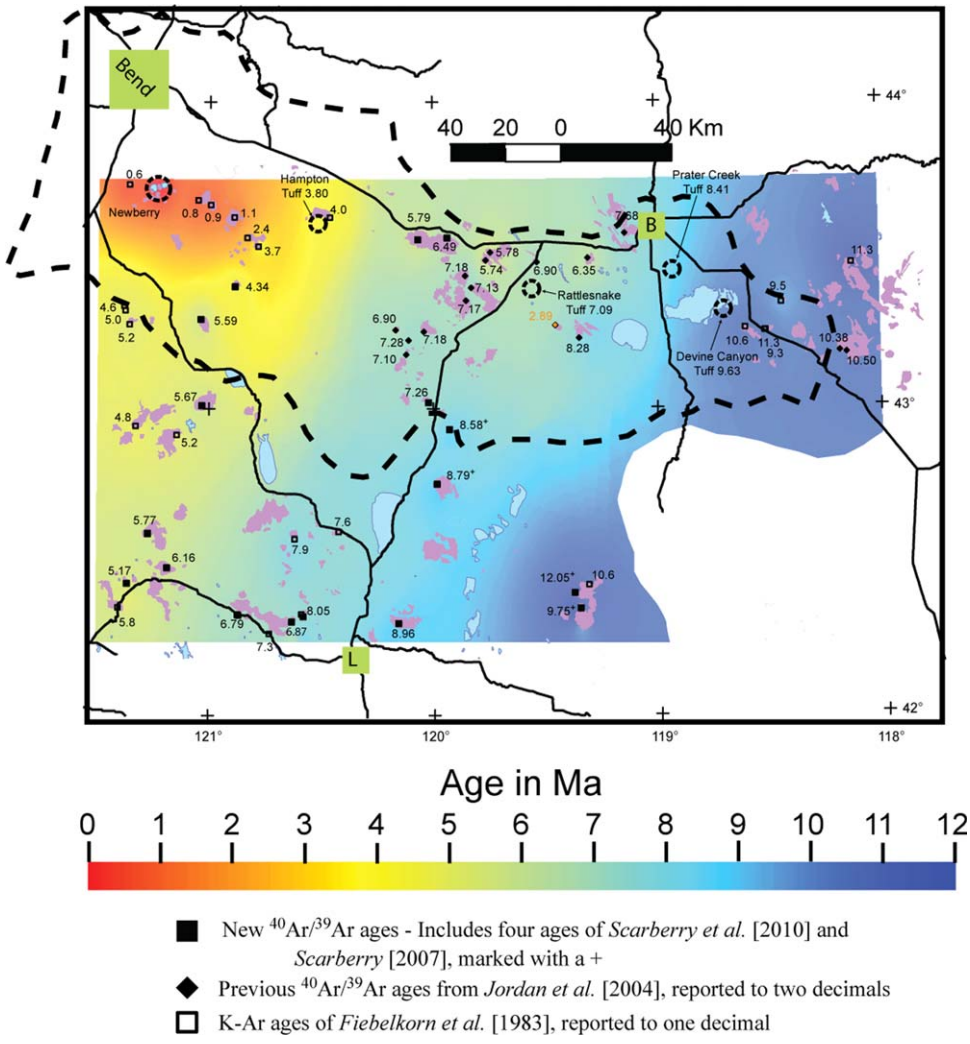

Figure 5. Map with a stretched color ramp of interpolated ages over much of the study area, with HLP and NWBR silicic centers in purple. Known ages (Table 1, Table S1) <12 Ma represented (see key). Coloring indicates age and was created by an IDW stretched color ramp. White space indicates that there was not sufficient data for interpolation. Green boxes are towns (B = Burns, L = Lakeview), heavy dashed line outlines physiographic HLP (Figure 1) and black lines are major roads. Proposed location for the RST source from *Streck and Grunder*, [1997] and proposed locations of vents, based in part from this map, field evidence and Grunder (unpublished) for other tuffs (Hampton, Prater Creek, and Devine Canyon) shown with dashed circles. $^{40}Ar/^{39}Ar$ age for the Hampton Tuff is from *Iademarco* [2009]. The following points were removed for this interpolation: The Deschutes Formation-aged 6.25 Ma Pine Mountain (Figure 3c) and 6.8 Ma China Hat and the 2.89 Ma Iron Mountain (shown in yellow text).

suggest viscous flow. The latter three are a considerable distance from reasonable roadways and were originally mapped as rhyolite [*Walker and MacLeod*, 1991] but when field checked they were determined to be basalt or basaltic andesite.

4. Discussion

4.1. Age Progressive Volcanism

[29] Our new ages increase the density of data, refine and support the westward-younging age progression of rhyolite centers in the HLP volcanic province established by *MacLeod et al*. [1976] and modified by *Jordan et al*. [2004] and expand the range of this age distribution to unequivocally include the NWBR. We have applied an inverse distance (squared) weighted (IDW), stretched color ramp (IDW interpolation: *Shepard* [1968] and *Naoum and Tsanis* [2004]) to the age determinations to create a color-coded map (Figure 5). This illustrates that the west-northwest younging pattern applies to silicic rocks in the HLP-NWBR as far south as the California border, and that these rhyolites constitute a single, age-progressive volcanic province that has been active over the past 12 Ma

[30] Although the isochrons of *Jordan et al*. [2004] display the westward sweep of silicic volcanism, our graduated interpolation has the advantage of not forcing a particular isochron through the data, therefore reducing the number of apparent misfits, and shows the age progression as a more systematic sweep than as depicted by the isochrons. It should be noted that one limitation of the IDW interpolation is the radial symmetry [*Watson and Philip*, 1985] or "halo" effect created by some isolated data points (e.g., the 9.5 Ma K-Ar age in the eastern HLP). However, despite the proclivity for the IDW interpolation to highlight anomalous ages, there are enough consistent data within the HLP-NWBR system to discern a broadly WNW volcanic transgression.

[31] Excluded from this analysis are two older episodes of silicic volcanism that crop out in the area, (1) the 38.5–20 Ma, region-wide events of subduction-related calc-alkaline John Day volcanism [*Robinson et al*., 1990] and (2) silicic volcanism coeval with the Steens Basalt lava flows episode, generally 17.5–15 Ma. Exposures of John Day-aged volcanism crop out at the margins of the HLP volcanism or in scarps created by Basin and Range faults within the NWBR [cf., *Iademarco*, 2009; *Scarberry et al*., 2010]. A few paleotopographic highs of Steens-age felsic volcanic rocks occur in both the HLP (e.g., Horsehead and Little Juniper Mountain, *Jordan et al*. [2004]) and in the NWBR (e.g., Bald Butte and Drum Hill, Table 1; Hawks Mountain, *Brueseke et al*. [2008]). Additional Steens-age felsic volcanic rocks lie east and south of the <12 Ma HLP-NWBR volcanic province described here.

[32] Only two of the <12 Ma rhyolitic lavas do not conform to the westward age sweep. One is Iron Mountain, which has an age of 2.89 ± 0.16 Ma, but lies in an area of rhyolitic volcanism that is about 7 Ma [*Jordan et al*., 2004] (Figure 5). We interpret this center to be part of the HLP, but it is clearly a postage-progressive rhyolite and may be associated with a pulse of young basaltic activity that extends along the length of the HLP. Iron Mountain is analogous to post rhyolite-sweep centers in the eastern Snake River Plain that are associated with younger basaltic volcanism (e.g., Big Southern Butte, Cedar Butte, East Butte; *McCurry et al*. [2008]). In contrast, there are no silicic centers in the NWBR younger than the age progression. The NWBR also lacks a distinct pulse of younger (<3 Ma) basaltic volcanism although there may be a few isolated young basalt flows.

[33] The 6.25 ± 0.03 Ma low-silica rhyolite at Pine Mountain crops out in an area where the age trend would indicate rhyolitic volcanism be <1 Ma (Figure 3c). Pine Mountain is similar in age to the low-silica rhyolite at Cline Buttes located about 60 km away and the rhyodacite of Steelhead Falls of the Deschutes Formation, which are related to Cascades volcanism [*Sherrod et al*., 2004] and we believe this to be the southeastern-most exposure of this formation, although further study is needed. A K-Ar age of 22.0 ± 4 Ma [*Fiebelkorn, et al*., 1983] is reported from a sample on the flanks of the mountain, indicating multiple episodes of volcanism older than the age progression are exposed at this location, one possibly correlative to the Deschutes Formation and the other to the John Day Formation. China Hat dome, located just south of Pine Mountain, has published K-Ar dates of 6.3 ± 1.1 and 7.4 ± 0.8 Ma (Table S1; *Fiebelkorn et al*. [1983]), indicating that there could be other Deschutes Formation rhyolites in this area. Neither of the Deschutes aged centers or Iron Mountain are included in the determination of the color ramp for Figure 5.

[34] When combined, the HLP and NWBR show a 12–0 Ma sweep of volcanism across Oregon but eruption rates vary across the province. Voluminous tuffs (RST, PCT, and DCT) erupted only from the HLP and only between 10 and 7 Ma, and accounted for well over half of the total volume of silicic volcanic rocks. A further difference between the two subprovinces is that HLP activity occurred over the entire 12–0 Ma time span whereas the NWBR does not contain rhyolites younger than about 5 Ma. Finally, the age color ramp map (Figure 5) reveals several gaps of >1 Ma in the rhyolite ages, or at least gaps in rhyolite exposures, within the HLP including the intervals from 9.6 to 8.4, 8.2 to 7.3, and 5.8 to 4.34 Ma. The NWBR has substantially fewer dated samples but there are no gaps in dated rhyolite exposures >0.75 Ma. These larger gaps in rhyolite ages in the HLP may be due to lulls in rhyolitic activity or may be a result of younger cover in basins or by basalt flows. Each of these possibilities is discussed later.

4.1.1. Basal—Rhyolite Connection and Timing of Volcanism

[35] Inasmuch as a flux of basalt is required as either a thermal or material source for rhyolitic magma production [e.g., *Hildreth*, 1981; *Huppert and Sparks*, 1988; *Nekvasil et al*., 2000], the 12–0 Ma basalts of the HLP-NWBR do not make an age sweep comparable to the rhyolites and instead

occur in episodes. We examine the link between the timing of basaltic pulses and rhyolite production, primarily in the HLP, first looking at cases where there may be a temporal link and then at periods where no such link is evident. In some cases, basaltic magmas may be stalled in the crust (intraplated) if regional tectonics or crustal lithology (density) are not conducive to eruption, similar to the conditions inferred for some basalts of the Snake River Plain [*McCurry and Rodgers*, 2009]. In other cases, the related basalts may simply be covered by younger volcanic rocks or, in the case of the Harney Basin, located only in the subsurface due to basin subsidence.

[36] Basaltic magmas erupted widely across much of the HLP from 7.8 to 7.5 Ma [*Jordan et al*., 2004]. This pulse was soon followed by voluminous rhyolite volcanism within the HLP from 7.3 to 6.9 Ma, including many domes and the 280 km^3 RST at 7.1 Ma [*Streck and Grunder*, 1995; *Jordan et al*., 2004], representing approximately a quarter of the total volume of silicic magmatism (Figure 3d). In part, the basaltic flows and voluminous RST may well have covered rhyolitic lavas erupted coeval with basaltic lavas or there may have been a thermal lag between basalt and rhyolite activity [*Jackson et al*., 2003]. Furthermore, there are limited basalts in the NWBR but still some silicic centers within the NWBR that fall within this age range (Figure 5). The spatial relationships of basalt to rhyolite eruption and the delay between the two, however, demonstrates that basalt eruption is not directly coupled to rhyolitic volcanism, as the geographic extent of the 7.8–7.5 Ma basalts are not accompanied by a similar distribution of rhyolites or, alternatively, the 7.3–6.9 Ma flare-up of rhyolitic volcanism is not accompanied by widespread basaltic volcanism. Regardless, there is a pulse of basaltic activity that just predates rhyolitic volcanism including a large-volume tuff.

[37] *Jordan et al*. [2004] also postulated a small pulse of basaltic volcanism between 5.9 and 5.3 Ma which is restricted to the western part of the HLP-NWBR border. This increased activity is coeval with or slightly older than nearby rhyolitic volcanism (e.g., Hagar Mountain, North Connelly Hills, Yamsay Mountain; Figure 3d and Table 1). Due to the paucity of basalt ages within the NWBR, it is not clear if mafic volcanism of this age extends throughout the province and relates to the 6–5 Ma rhyolitic volcanism in the NWBR, so the correlation is weak.

[38] Another, less pronounced pulse of basaltic volcanism occurred province wide from 3 to 2 Ma [*Jordan et al*., 2004]. While extending the length of the HLP, this pulse is not represented in the NWBR and is smaller and more focused on the axis of the HLP compared to the pulse at ~7.5 Ma. The smaller overall volume suggests a general waning of the basaltic flux, but perhaps sufficient to produce rhyolite as indicated by the emplacement of the 2.8 Ma Iron Mountain. The closest basalt of a similar age crops out ~30 km away. Reduced rhyolitic activity at this time is also likely a result of the crust becoming more refractory due to continued injection (intraplating) of basaltic magma and mafic residuum from earlier rhyolite production [*Ford and Grunder*, 2011]. While there are no young basalts in the NWBR, there are also no rhyolites <4 Ma either.

[39] A correlation between basaltic volcanism and the older set of voluminous tuffs (PCT at 8.4 Ma and DCT at 9.63 Ma), which account for approximately a quarter of the rhyolitic volcanism, is more difficult to establish. Basalts of a broadly similar age are associated with the ~10.5 Ma emplacement of the Duck Butte Eruptive Center [Johnson and Grunder, 2000], Malheur caves area [*Jordan et al*., 2004], and the 12–9 Ma "Southern Harney Basin Group" [*Brown et al*., 1980] which is south of the proposed source location of the DCT (Figure 3d). In addition to these basalts, the more widely distributed ~12.5–10 Ma Keeney Sequence flows crop out <45 km east of the source of the DCT [Hooper et al., 2002; *Camp et al*., 2003]. Only one basalt of this age crops out in the NWBR [*Scarberry et al*., 2010]. Other basalts that might have been erupted near the time of the PCT and DCT eruptions are relegated to the subsurface in the Harney Basin, as basalt-sediment interbeds extend to depths >1000 m in many places [*Newton et al*., 1962; *Milliard*, 2010]. Much of this sediment was deposited after the rapid onset of subsidence in the basin starting at approximately 10 Ma and ending or slowing significantly by the time of the emplacement of the 7.25 Ma Drinkwater basalt [*Milliard*, 2010]. Additionally, the voluminous PCT and DCT and younger lava flows and sediment may cover many basalt flows that are related to this period. An alternative which cannot be disproved with current information is that due to different tectonic stresses at this time, basalts associated with these rhyolites did not erupt to the same degree as younger basalts. It is unclear if basalt "bedrock" encountered in the well logs at depth is part of the middle Miocene Steens Basalt lava flows or a

younger, "HLP-aged" flow. Either there are no basaltic flows associated with voluminous rhyolitic eruptions of this time, or they are only sparsely exposed at the surface.

[40] The most recent pulse of HLP-wide basaltic volcanism spans the past 50 ka. While much of this young basaltic volcanism is centered around Newberry Volcano and to the east of Newberry (e.g., Potholes, Devils Garden flows) [*Jordan et al*., 2004; *Jenson*, 2006], some young volcanism occurs well to the east in the HLP volcanic province, including Diamond Craters [*Russell and Nicholls*, 1987; *Sherrod et al*., 2012] and Jordan Craters [*Otto and Hutchison*, 1977; *Hart and Mertzman*, 1983]. No young basalts of this age are present in the NWBR based on flow morphologies and age determinations. Except for Holocene rhyolites at Newberry Volcano (e.g., Big Obsidian Flow), there are no rhyolites associated with this youngest pulse of basaltic activity. We attribute this to a combination of insufficient flux of mafic magmas and a crust that has been made too refractory for partial melting [*Ford and Grunder*, 2011], or the thermal lag between basalt and rhyolite activity [*Jackson et al*., 2003].

[41] In all of the above cases, there is either a spatial or temporal decoupling between the eruptions of basalts and rhyolites. For the 7.8–7.5 Ma pulse, regional tectonic events (e.g., initiation of the High Cascades, a change in Pacific Plate motion) likely triggered deformation and the widespread eruption of basalts that is strongly concentrated in the HLP, as discussed in *Jordan et al*. [2004]. It is unclear if localization of crustal stresses created pathways for basaltic magmas to reach the surface or if increased melt volumes in the crust reduced rock strength to facilitate faulting [*Rosenberg et al*., 2007]. At this time, NWBR has a kinematic link to the Brothers Fault Zone in the HLP [*Trench et al*., 2012]. By the time of the 5.9–5.3 basaltic pulse, *Trench et al*. [2012] propose a decoupling of the kinematic link between the HLP and NWBR, resulting in an independent slip history for the HLP and a reduction in deformation rates. This could be the reason that the 3–2 Ma and $<$50 ka basaltic pulses are relegated to the HLP whereas the $\sim$7.5 Ma pulse covered a greater area. The mantle-derived injections that drive silicic magmatism are decoupled from the basaltic eruptions, which reach the surface based on local or regional transtension.

4.1.2. Subsidence of the HLP and Effects on Rhyolite Outcrop Distribution

[42] The geomorphic expression of the HLP is an elongate trough with generally muted topography, similar to the Snake River Plain. Areas with few rhyolite domes exposed reflect apparent age gaps in volcanic activity in the HLP. The Harney Basin has a gap from 9.6 to 7.3 Ma with only one dome exposed within that range, and the area south of Frederick Butte has a gap from 5.8 to 4.34 Ma (Figure 3d and 5). The paucity of rhyolitic lavas between 9.6 and 7.3 Ma in the Harney Basin we attribute to cover by younger volcanic rocks and sediments resulting from subsidence of the HLP, a consequence of persistent injection of basalts into the crust. The paucity of rhyolites of 5.8–4.34 Ma age is partly a result of cover by younger volcanic rocks ($\pm$ limited sediment), especially on the flanks of Newberry Volcano, but may also reflect a change in regional tectonics. These processes are briefly explored later.

[43] The dips into the basin on tuffs along the northern margin of the Harney Basin increase with increasing age, so that the 9.6 Ma DCT has a dip of 6°, the 8.4 Ma PCT dips at 3° and the 7.1 Ma RST dips $<\sim$1° [Milliard, 2010]. The changes in dip were not caused by any uplift in the adjacent Blue Mountains province within the past 10 Ma [*Walker and Robinson*, 1990]. Broad, gentle folds located along the southern margin of the Harney Basin in RST-aged volcanic rocks are in-filled with 6.1 Ma (K-Ar age) flat-lying basaltic flows and plunge toward the center of the basin [*Brown et al*., 1980].

[44] The Harney Basin region has experienced downward crustal flexure or sag similar to that of the Snake River Plain [*McQuarrie and Rodgers*, 1998] with crustal loading due to mass transfer from the mantle to the crust via intraplated basaltic magmas, diking and volcanism, with additional mass added by basin sedimentation. Even shallow dips on units to the north and south of the basin could easily manifest multiple kilometers of crustal downwarping on the scale of the study area. The one dome that does crop out within this age range is Burns Butte, located on the northern edge of the Harney Basin (Figure 3d), where subsidence would be minimal. Recent geophysical studies [*Cox*, 2011] indicate volcanic rocks and sediments may extend to as deep as 7 km in the Harney Basin, at least 2 km deeper than other places in the HLP or Basin and Range. Well logs from the eastern part of the Harney Basin indicate 0.75 to more than 1.5 km of sediment [*Milliard*,

2010]. The timing of subsidence coincides with voluminous rhyolitic eruptions, and subsidence wanes after the focus of silicic volcanism moved westward.

[45] The lack of exposed silicic volcanism from 5.8 to 4.34 Ma in the western HLP likely has a different cause. There is an overall decline in silicic volcanic volume in the HLP-NWBR starting at this time. Activity ceased in the NWBR by 5 Ma, and in the HLP, rhyolites are constrained to a narrow band of small-volume domes on the eastern flank of the Newberry shield <3.7 Ma. There are no large dome complexes erupted on the HLP after the 5.7 Ma, 25–50 km^3 Glass Buttes. This would correspond to a significant decrease in basalt addition, and we consider it unlikely that the relatively small amounts of mass added to the crust in this area could cause downwarping.

[46] Extension via Basin and Range faults has propagated in episodic steps westward (and northward) across the NWBR over at least the past 10 Ma [*Scarberry, et al*., 2010]. This westward propagation into the Cascades corresponds with an increase in volcanic activity within the arc in central Oregon, just prior to 4.5 Ma [*Hughes and Taylor*, 1986]. This model is consistent with the marginward migration of basalt or bimodal basalt-rhyolite volcanism throughout the entire Basin and Range province and the general westward sweep of rhyolitic volcanism in the northern Basin and Range from 12 to 5 Ma [*Luedke and Smith*, 1984; *Fitton, et al*., 1991]. This transfer and reorganization of crustal stresses to the axis of the active arc may have greatly reduced either the formation of rhyolitic magmas or their ability to reach the surface in the HLP and NWBR. Also, Pliocene and younger basalt coverage is more extensive in this area than in other parts of the HLP, especially as one approaches the Newberry shield, and this may have covered some small-volume domes.

4.2. The HLP-NWBR Age Progressive Trend and Asthenospheric Flow, A Unifying Model

[47] An unresolved question is, what has caused the age progressive volcanism in the HLP and NWBR? We propose that the volcanism in the HLP and NWBR is a result of Cascadia slab plate-driven asthenospheric flow and does not require a mantle plume. Surface expression of HLP rhyolitic volcanism moves approximately N20°W at ~33 km/Ma, from 12 Ma until 4 Ma (Figure 6) [*Jordan et al*., 2004] and the North American Plate moves S40°W at ~26 km/Ma [*Gripp and Gordon*, 2002]. Simple vector addition of North American plate motion and the HLP age-progressive rhyolitic volcanism trend very closely matches the direction of asthenospheric flow, as recently determined by shear wave splitting (SKS phases) delay times [*Long et al*., 2009] (Figure 6). The calculated asthenospheric flow is ~53 km/Ma, which is consistent with the magnitude of the *S* wave delay times, some of the largest recorded, indicating very strong anisotropy and alignment in the asthenosphere [*Long et al*., 2009]. Additionally, young basalts from the HLP have $He/^4He$ values of 8.8–9.3 R_A, which are within the range of mid-ocean basalts and do not indicate a plume component [*Graham et al*., 2009].

[48] Many subduction zones are dominated by trench parallel flow (toroidal edge flow) or show heterogeneous flow vectors [e.g., *Long and Silver*, 2008] but the flow vectors under the HLP are nearly unidirectional (Figure 6d) [*Long et al*., 2012]. Other workers using three-dimensional strain modeling [*Druken et al*., 2011; *Long et al*., 2012] have recently shown that the downdip only motion (Figure 7) on the Cascadia slab is insufficient to create the mantle wedge flow observed under Oregon and thus a combination of trench rollback, slab steepening, and back-arc extension is required to produce the seismic anisotropy observed. Downdip motion alone only produces weak corner flow and little upwelling from the mantle.

[49] Geodynamical models from Long et al. [2012] require modest back-arc extension to draw material from depth to give the thermal modeling results. But, they do not separate trench rollback induced anisotropy from that related to slab steepening. Long et al. 's [2012] results also show that mantle flow is focused inboard (northward) of the slab edge a considerable distance in the slab rollback, steepening and backarc extension models. Other workers have shown that the southern portion (that portion under Oregon and northern California) of the Cascadia slab is coherent and is not fragmented until it reaches the transition zone (>410 km) [*Roth et al*., 2008; *James et al*., 2011] and thus a shallow fragmented slab does not produce the mantle upwelling required in this region.

[50] The southern Cascadia slab is subducting at a steeper angle than the portion under Washington State (Figure 7). This is based on the trench to arc

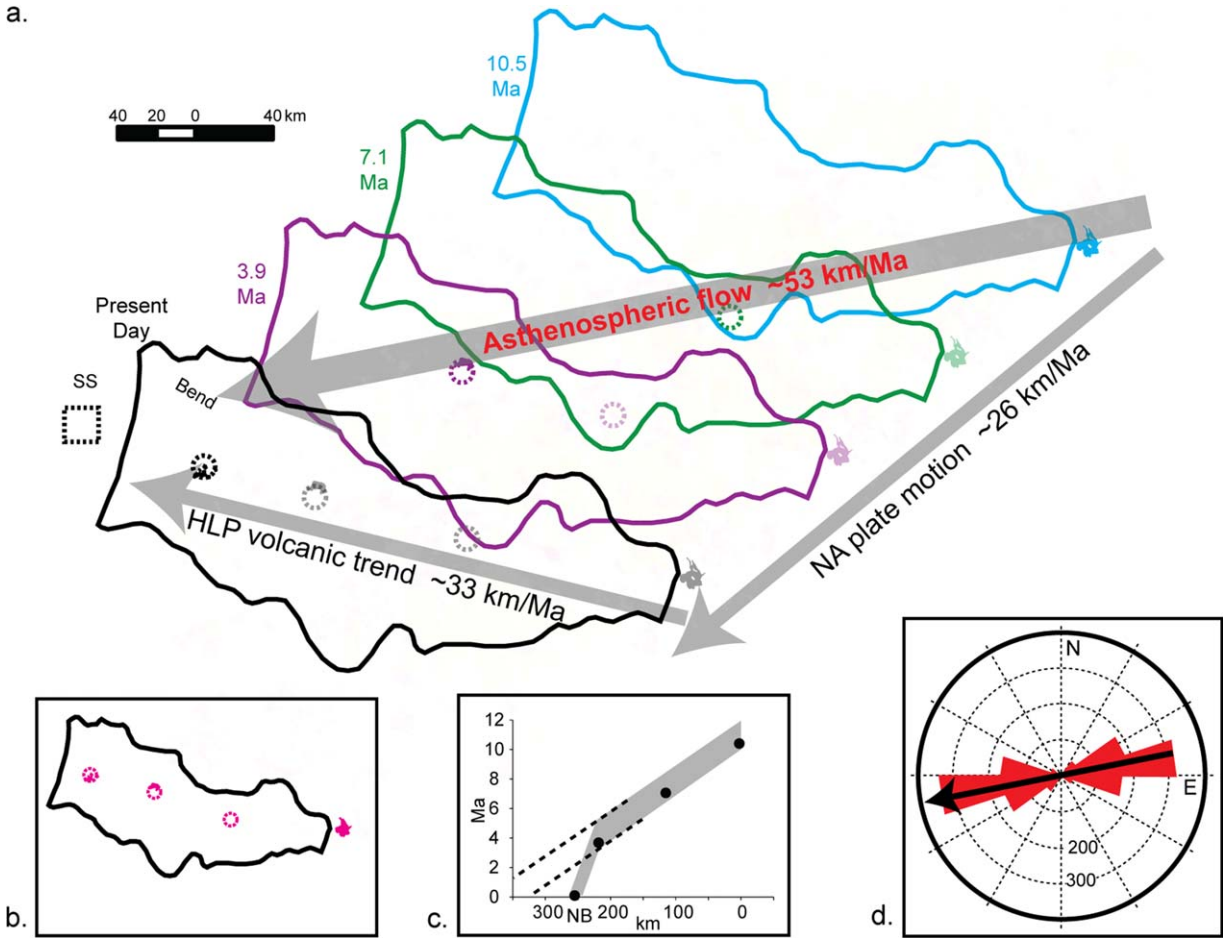

Figure 6. Resolving asthenospheric flow and plate motion to create the HLP volcanic trend. (a) Four time slices at 10.5 (Duck Creek Butte), 7.1 (RST), 3.9 (Frederick Butte and Hampton Tuff), and 0 Ma (Newberry Volcano, present day) showing the positions of subsequent eruptions with the motion of the North American Plate (26 km/Ma) Colors for eruptions from previous time slices are muted. Figure is to scale indicating westward asthenospheric flow rate is generally uniform, averaging 53 km/Ma from 10.5 to 4 Ma. (b) A simplified geologic map of the HLP showing only the four age-progressive eruptions discussed (compare to Figure 3d). (c) Surface expression of HLP rhyolitic volcanism moves WNW at ~33 km/Ma [after *Jordan et al*., 2004] but the rate slows at ~4 Ma (see text). The four episodes discussed are plotted (NB = Newberry Volcano). Dotted box in Figure 6a indicates where volcanism would plot if the HLP volcanic trend rate had remained at 33 km/Ma, approximately 25 km south of South Sister Volcano (SS) in the Cascades. (d) A histogram showing shear wave splitting (SKS phases) delay times for the HLP [*Long et al*., 2009] with black arrow from this calculation of asthenospheric flow from Figure 6a.

distance, if volcanism occurs at the same depth above the slab along the arc [cf., *Hildreth*, 2007], the location of the shallow slab based on earthquake locations and depths [*McCrory et al*., 2012] and *P* wave tomographic results [*Roth et al*., 2008; *Pavlis et al*., 2012]. Slab steepening is also suggested as the southern portion of the slab is unsupported [e.g., *Zandt and Humphreys*, 2008]. Slab steepening could also result in enhanced horizontal mantle alignment.

[51] The progressive steepening of the slab from north to south may focus the increased asthenospheric counterflow or upwelling to a more narrow band, which results in the HLP track. This focused flow results in a greater flux of basaltic magmas to drive silicic magmatism and resulted in intraplated basalts and mafic residuum, a process we term "basaltification." This basaltification, especially in the Harney Basin area, produced crustal flexure and helped shape the overall topography of the region. Partial melts of the increasingly mafic crust in the HLP produced the iron-rich rhyolites whereas rhyolites of the NWBR are lower in iron [*Ford*, 2012]. This combination of focusing of asthenospheric flow resulting from the downgoing slab and possibly lithospheric permeability in the HLP results in the enhanced volcanism along the

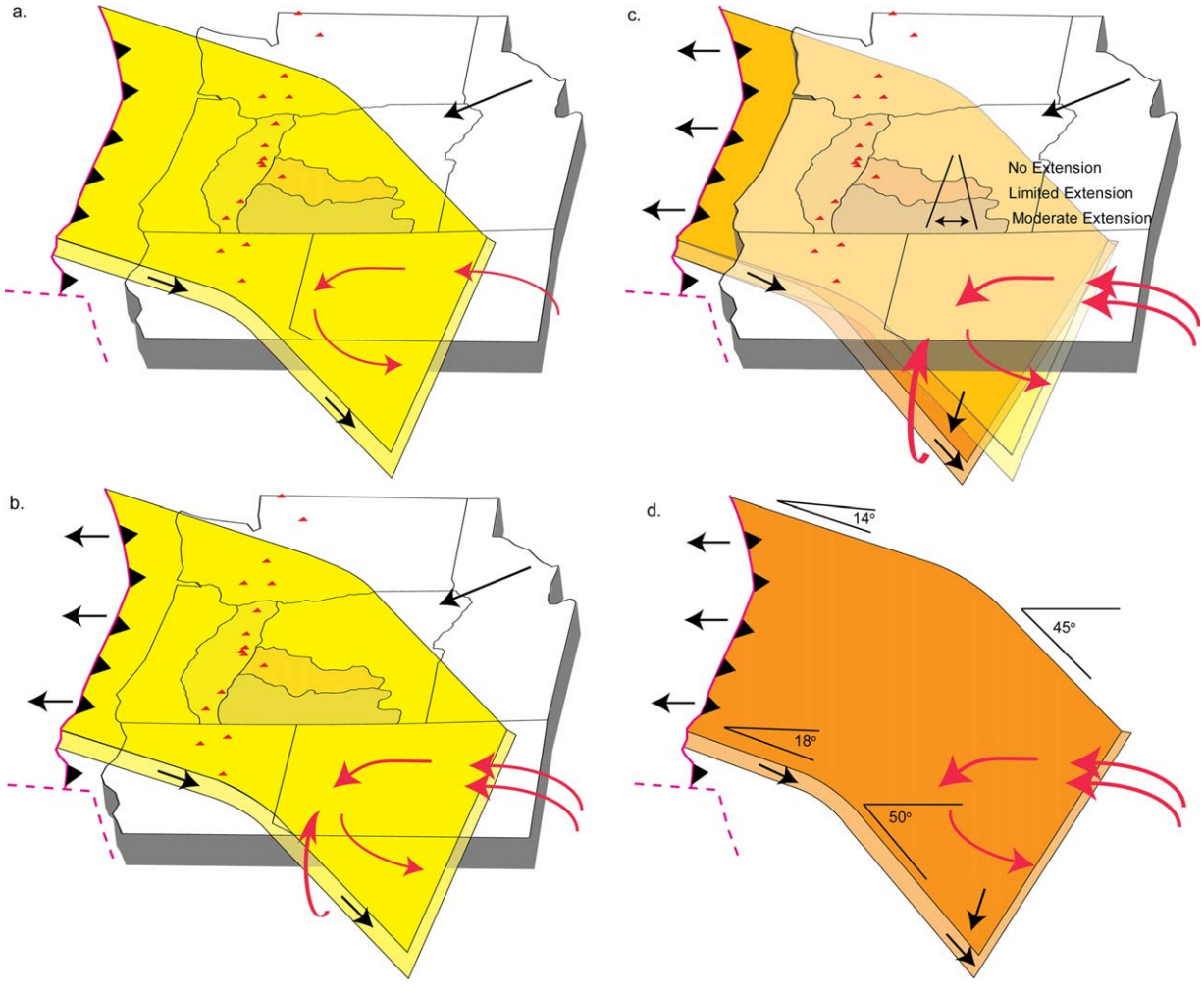

Figure 7. Schematic models (nearly to scale and with approximately no vertical exaggeration) of the processes that drive mantle upwelling and counterflow as a result of the subducting Cascadia slab. Plate motions are shown with black arrows and mantle flow with red arrows. Red triangles are the current day locations of Cascade volcanoes and the Cascades, HLP, and NWBR physiographic provinces are outlined (Figure 1). The position of the trench and transform faults (red dotted line) are also shown. (a) Limited corner flow associated with downdip motion only, before trench rollback commenced. (b) Slab rollback initiates a much stronger mantle flow as North America continues to advance on the trench. (c) The addition of slab steepening due to the southern edge of the slab being unsupported can further enhances this flow, which is concentrated under the HLP. Differing extensional rates in the continental slab (crustal factors) may also play a role in the volcanic expression. The current geometry of the Cascadia slab is shown in orange. (d) Simplified version of Figure 7c showing the current Cascadia slab only. Angles given are approximate and taken from *McCrory et al*. [2012] and *Roth et al*. [2008] and the slab steepens markedly at the volcanic front (~100 km depth) [*Pavlis et al*. 2012].

HLP. While there is very little crustal extension in the HLP [*Meigs et al*., 2009; *Trench et al*., 2012], it is still greater than that in the adjacent Blue Mountains (Figure 7).

[52] We also observe that basalts trend to higher MgO/(MgO+FeO*) through time [*Ford*, 2012], so that younger basalts are hotter than older basalts, regardless of E-W location in the HLP. This indicates that the parental basaltic magmas to this system might be changing through time, toward hotter basaltic magmas and greater degrees of partial melting of the mantle, a changing asthenospheric source composition or interaction with a more depleted mantle lithosphere [cf., *Carlson and Hart*, 1987]. Modeling of thermal anomalies using trench rollback and extension in the backarc also indicates that mantle temperatures should increase over time [*Long et al*., 2012]. In our model, slab rollback, back-arc extension, and the progressive steepening of the slab to the north results in enhanced counterflow (Figure 7) and a plume in not a necessary heat source. We favor an

enhanced flow in the mantle to generate the volumetrically superior HLP while lithospheric processes may play a larger role in the related volcanism of the NWBR, due to substantially greater amounts of crustal extension.

[53] If the HLP volcanic trend continued to move at 33 km/Ma, instead of appearing to slow at about 4 Ma, the current location of volcanic activity would be at the apex of the Cascade range, approximately 25 km south of South Sister volcano [cf., *Hill and Taylor*, 1989; *Jordan et al*., 2004] (Figure 6). The highest density of volcanic vents in the Oregon Cascades and very young (<40 ka) silicic centers are found in the Three Sisters Volcanic Field [*Guffanti and Weaver*, 1988; *Schmidt and Grunder*, 2011], which is at the intersection of the HLP trend and the Cascades graben.

5. Conclusions

[54] We extend the westward age progression of rhyolites in the HLP to include the NWBR and describe a single, age-progressive volcanic sweep that extends from the margin of the Blue Mountains Terrane to the California border and from the Steens escarpment to the flanks of the Newberry shield. This bimodal province, with equal erupted volumes of basalt and rhyolite, has been active over the past 12 million years, continuing in the HLP until the present. Basaltic eruptions often occur in pulses and are decoupled from the age-progressive rhyolites. Basin subsidence, driven by a process similar to that invoked for the Snake River Plain [*McQuarrie and Rodgers*, 1998], and caused by dense intraplated basaltic magmas and residuum from partial melting, has likely buried some silicic centers in the subsurface (such as in the Harney Basin). The transfer and reorganization of crustal stresses to the axis of the active arc by the formation of the northward-opening Cascades graben [*Smith et al*., 1987; *Conrey et al*., 1997] may have terminated volcanic activity in the NWBR and led to waning of rhyolitic volcanic activity in the HLP <4 Ma while increasing activity in the Three Sisters area of the Cascades. The westward asthenospheric flow required to produce the HLP volcanic trend, given the southwestward North American Plate motion, is nearly identical to seismically imaged flow [*Long et al*., 2009], and this motion has been reproduced in laboratory tank models [*Druken et al*., 2011]. The only geodynamic feature required to produce this mantle flow is the downgoing Cascadia slab; no plume is required. Volcanism in the HLP and NWBR is driven by this flow and focused in the HLP due to slab rollback, steepening and back-arc extension.

Acknowledgments

[55] This work is part of the High Lava Plains Project, with support provided by the NSF Continental Dynamics program through grant EAR-0506869 (ALG and RAD). We thank Layne Bennett and Darrick Boschmann for GIS assistance and the VIPER (Volcanology, Igneous Petrology and Economic Research) group at Oregon State University for discussion. We would also like to thank Matt Brueseke, Gail Mahood and Rick Carlson for their insightful and thoughtful reviews of this paper.

References

Bestland, E. A., and G. J. Retallack (1994a), Geology and paleoenvironments of the Clarno Unit, John Day Fossil Beds National Monument, Oregon, *U. S. Natl. Park Syst. Open File Rep.,* 160 pp.

Bestland, E. A., and G. J. Retallack (1994b), Geology and paleoenvironments of the Painted Hills Unit, John Day Fossil Beds National Monument, Oregon, *U. S. Natl. Park Syst. Open File Rep.*, 211 pp.

Boschmann, D. (2012), Structural and volcanic evolution of the Glass Buttes Area, High Lava Plains, Oregon, M.S. thesis, 100 pp., Oreg. State Univ., Corvallis.

Brikowski, T. H. (1983), Geology and petrology of Gearhart Mountain: A study of calc-alkaline volcanism east of the Cascades in Oregon, Ph.D. thesis, 157 pp., Univ. of Oreg., Eugene.

Brown, D. E., G. D. McLean, and G. L. Black (1980), Preliminary geology and geothermal resource potential of the southern Harney Basin, Oregon, *Oreg. Dep. Geol. Miner. Ind. Open File Rep. O-80-07*, 90 pp.

Brueseke, M. E., W. K. Hart, and M. T. Heizler (2008), Diverse mid-Miocene silicic volcanism associated with the Yellowstone-Newberry thermal anomaly, *Bull. Volcanol.*, *70*, 343–360, doi:10.1007/s00445-007-0142-5.

Camp, V. E., and M. E. Ross (2004), Mantle dynamics and genesis of mafic magmatism in the intermontane Pacific Northwest, *J. Geophys. Res.*, *109*, B08204, doi:10.1029/2003JB002838.

Camp, V. E., M. E. Ross, and W. E. Hanson (2003), Genesis of flood basalts and Basin and Range volcanic rocks from Steens Mountain to the Malheur River Gorge, Oregon, *Geol. Soc. Am. Bull.*, *115*, 105–128, doi:10.1130/0016–7606.

Carlson, R. W., and W. K. Hart (1987), Crustal genesis on the Oregon Plateau, *J. Geophys. Res.*, *92*, 6191–6206. doi:10.1029/JB092iB07p06191.

Christiansen, R. L., G. R. Foulger, and J. R. Evans (2002), Upper-mantle origin of the Yellowstone hotspot, *Geol. Soc. Am. Bull.*, *114*, 1245–1256, doi:10.1130/0016–7606(2002)114<1245:UMOOTY>2.0.CO;2.

Coble, M. A., and G. A. Mahood (2012), Initial impingement of the Yellowstone plume located by widespread silicic volcanism contemporaneous with Columbia River flood basalts, *Geology*, *40*, 655–658, doi:10.1130/G32692.1.

Conrey, R. M., D. R. Sherrod, P. R. Hooper, and D. A. Swanson (1997), Diverse primitive magmas in the Cascade arc,

northern Oregon and southern Washington, *Can. Mineral.*, *35*, 367–396.

Cox, C. (2011), A controlled-source seismic and gravity study of the High Lava Plains (HLP), M.S. thesis, 110 pp., Univ. of Okla., Norman.

DeMets, C., R. G. Gordon, D. F. Argus, and S. Stein (1994), Effect of recent revisions to the geomagnetic reversal time scale on estimate of current plate motions, *Geophys. Res. Lett.*, *21*, 2191–2194, doi:10.1029/94GL02118.

Dicken, S. N. (1950), *Oregon Geography*, 1st prelim. ed., Edwards Brothers, Ann Arbor, Mich., 104 pp.

Donnelly-Nolan, J. M., D. E. Champion, C. D. Miller, T. L. Grove, and D. A. Trimble (1990), Post-11,000-year volcanism at Medicine Lake Volcano, Cascade Range, northern California, *J. Geotherm. Res.*, *95*(B12), 19,693–19,704.

Donnelly-Nolan, J. M., T. L. Grove, M. A. Lanphere, D. E. Champion, and D. W. Ramsey (2008), Eruptive history and tectonic setting of Medicine Lake Volcano, a large rear-arc volcano in the southern Cascades, *J. Volcanol. Geotherm. Res.*, *177*, 313–328, doi:10.1016/j.jvolgeores.2008.04.023.

Draper, D. S. (1991), Late Cenozoic bimodal magmatism in the northern Basin and Range Province of southeastern Oregon, *J. Volcanol. Geotherm. Res.*, *47*, 299–328, doi:10.1016/0377-0273(91)90006-L.

Druken, K. A., M. D. Long, and C. Kincaid (2011), Patterns in seismic anisotropy driven by rollback subduction beneath the High Lava Plains, *Geophys. Res. Lett.*, *38*, L13310, doi:10.1029/2011GL047541.

Duncan, R. A., and L. G. Hogan (1994), Radiometric dating of young MORB using the 40Ar-39Ar incremental heating method, *Geophys. Res. Lett.*, *21*(18), 1927–1930, doi:10.1029/94GL01375.

Duncan, R. A., and R. A. Keller (2004), Radiometric ages for basement rocks from the Emperor Seamounts, ODP Leg 197, *Geochem. Geophys. Geosyst.*, *5*, Q08L03, doi:10.1029/2004GC000704.

Duncan, R. A., P. R. Hooper, J. Rehacek, J. S. Marsh, and A. R. Duncan (1997), The timing and duration of the Karoo igneous event, southern Gondwana, *J. Geophys. Res.*, *102*, 18,127–18,138, doi:10.1029/97JB00972.

Eungard, D. W. (2012), Early High Cascades silicic volcanism: Analysis of the McKenzie Canyon and Lower Bridge Tuff, M.S. thesis, 273 pp., Oreg. State Univ., Corvallis.

Evans, S. H., and F. H. Brown (1981), Summary of potassium/argon dating-1981, *Department of Energy, Division of Geothermal Energy ID-12079-45*, 29 pp.

Fiebelkorn, R. B., G. W. Walker, N. S. MacLeod, E. H. McKee, and J. G. Smith (1983), Index to K-Ar determinations for the state of Oregon, *Isochron West*, *37*, 3–60.

Fitton, J. G., D. James, and W. P. Leeman (1991), Basic magmatism associated with late Cenozoic extension in the western United States: Compositional variations in space and time, *J. Geophys. Res.*, *96*, 13,693–13,711, doi:10.1029/91JB00372.

Ford, M. T. (2012), Rhyolitic magmatism of the High Lava Plains and adjacent northwestern Basin and Range, Oregon: Implications for evolution of the continental crust, Ph.D. thesis, 314 pp., Oreg. State Univ., Corvallis.

Ford, M. T., and A. L. Grunder (2011), Compositional trends in High Lava Plains and Northwest Basin and Range rhyolites, comparisons to Snake River Plain, Cascades and Iceland: Partial melt, fractionation, or both?, *Geol. Soc. Am. Abstr. Programs*, *43*(4), 5.

Graham, D. W., M. R. Reid, B. T. Jordan, A. L. Grunder, W. P. Leeman, and J. E. Lupton (2009), Mantle source provinces beneath the Northwestern USA delimited by helium isotopes in young basalts, *J. Volcanol. Geotherm. Res.*, *188*(1-3), 128–140, doi:10.1016/j.jvolgeores.2008.12.004.

Green, R. C. (1973), Petrology of the welded tuff of Devine Canyon, southeastern Oregon, *U.S. Geol. Surv. Prof. Pap. 797*, 1–26.

Gripp, A. E., and R. G. Gordon (2002), Young tracks of hotspots and current plate velocities, *Geophys. J. Int.*, *150*, 321–361, doi:10.1046/j.1365-246X.2002.01627.x.

Guffanti, M. M., and G. S. Weaver (1988), Distribution of Late Cenozoic volcanic vents in the Cascade Range: Volcanic arc segmentation and regional tectonic considerations, *J. Geophys. Res.*, *93*, 6513–6529, doi:10.1029/JB093iB06p06513.

Hart, W. K., and S. A. Mertzman (1983), Late Cenozoic volcanic stratigraphy of the Jordan Valley area, southeastern Oregon, *Oreg. Geol.*, *45*, 15–19.

Hart, W K., J. L. Aronson, and S. A. Mertzman (1984), Areal distribution and age of low-K, high-alumina olivine tholeiite magmatism in the northwestern Great Basin, *Geol. Soc. Am. Bull.*, *95*, 186–195. doi:10.1130/0016–7606(1984)95<186:ADAAOL>2.0.CO;2.

Heiken, G. H., R. V. Fisher, and N. V. Peterson (1978), A field trip to the maar volcanoes of the Fort Rock—Christmas Lake Valley basin, Oregon, *U. S. Geol. Surv. Circ. 838*, 1–28 pp.

Hering, C. W. (1981), Geology and petrology of the Yamsay Mountain Complex, south-central Oregon: A study of bimodal volcanism, PhD thesis, 189 pp., Univ. of Oreg., Eugene.

Hildreth, W. (1981), Gradients in silicic magma chambers: Implications for lithospheric magmatism, *J. Geophys. Res.*, *86*, 10,153–10,192, doi:10.1029/JB086iB11p10153.

Hildreth, W. (2007), Quaternary magmatism in the Cascades-Geologic perspectives, *U. S. Geol. Surv. Prof. Pap. 1744*, 125 pp.

Hill, B. E., and E. M. Taylor (1989), Oregon Central High Cascade pyroclastic units in the vicinity of Bend, Oregon, in *Guidebook for Field Trip to the Mount Bachelor-South Sister-Bend Area, Central Oregon High Cascades*, edited by W. E. Scott, C. A. Gardner, and A. M. Sarna-Wojcicki, *U. S. Geol. Surv. Open File Rep. 89-645*, 51–54.

Hooper, P. R., G. B. Binger, and K. R. Lees (2002), Ages of the Steens and Columbia River flood basalts and their relationship to extension-related calc-alkalic volcanism in eastern Oregon, *Geol. Soc. Am. Bull.*, *114*, 43–50, doi:10.1130/0016–7606(2002)114<0043:AOTSAC>2.0.CO;2.

Hughes, S. S., and E. M. Taylor (1986), Geochemistry, petrogenesis, and tectonic implications of central High Cascade mafic platform lavas, *Geol. Soc. Am. Bull.*, *97*, 1024–1036, doi:10.1130/0016–7606(1986)97<1024:GPATIO>2.0.CO;2.

Humphreys, E. D., K. G. Deuker, D. L. Schutt, and R. B. Smith (2000), Beneath Yellowstone: Evaluating plume and nonplume models using teleseismic images of the upper mantle, *GSA Today*, *10*, 1–7.

Huppert, H., and R. Sparks (1988), The generation of granitic magmas by intrusion of basalt into continental crust, *J. Petrol.*, *29*, 599–634, doi:10.1093/petrology/29.3.599.

Iademarco, M. J. (2009), Volcanism and faulting along the northern margin of Oregon's High Lava Plains: Hampton Butte to Dry Mountain, M.S. thesis, 141 pp., Oreg. State Univ., Corvallis.

Jackson, M. D., M. J. Cheadle, and M. P. Atherton (2003), Quantitative modeling of granitic melt generation and

segregation in the continental crust, *J. Geophys. Res.*, *108*(B7), 2332, doi:10.1029/2001JB001050.

James, D. E., M. J. Fouch, R. W. Carlson, and J. B. Roth (2011), Slab fragmentation, edge flow and the origin of the Yellowstone hotspot track, *Earth Planet. Sci. Lett.*, *311*, 124–135, doi:10.1016/j.epsl.2011.09.007.

Jensen, R. A. (2006), *Roadside Guide to the Geology and History of Newberry Volcano*, 4th ed., 182 pp., CenOreGeoPub, Bend, Oreg.

Jensen, R. A., J. M. Donnelly-Nolan, and D. Mckay (2009), A field guide to Newberry Volcano, Oregon, in *Volcanoes to Vineyards: Geologic Field Trips Through the Dynamic Landscape of the Pacific*, edited by J. E. O'Connor, R. J. Dorsey, and I. P. Madin, *Geol. Soc. Am. Field Guide, 15*, 53–79.

Johnson, J. A. (1995), Geologic evolution of the Duck Creek Butte eruptive center, High Lava Plains, southeastern Oregon, M.S. thesis, 151 pp., Oreg. State Univ., Corvallis.

Johnson, J. A. (1998), Geologic map of the Frederick Butte volcanic center, Deschutes and Lake counties, south-central Oregon, *U.S. Geol. Surv. Open File Rep. 98–208*, scale 1:40,000.

Johnson, M. J. (1984), Geology, alteration, and mineralization of a silicic volcanic center, Glass Buttes, Oregon, M.S. thesis, 129 pp., Portland State Univ., Portland, Oreg.

Johnson, J., and A. L. Grunder (2000), The making of intermediate composition magma in a bimodal suite: Duck Butte Eruptive Center, Oregon, USA, *J. Volcanol. Geothem Res.*, *95*, 175–195 doi:10.1016/S0377-0273(99)00125-0.

Johnson, K. E., and E. V. Ciancanelli (1984), Geothermal exploration at Glass Buttes, Oregon, *Geotherm. Res. Counc. Trans.*, *7*, 169–174.

Jordan, B. T. (2002), Basaltic volcanism and tectonics of the High Lava Plains, southeastern Oregon, Ph.D. thesis, 234 pp., Oreg. State Univ., Corvallis.

Jordan, B. T., M. J. Streck, and A. L. Grunder (2002), Bimodal volcanism and tectonism of the High Lava Plains, Oregon, in *Field Guide to Geologic Processes in Cascadia*, edited by G. W. Moore, *Oreg. Dep. Geol. Miner. Ind. Spec. Pap. 36*, 23–46.

Jordan, B. T., A. L. Grunder, R. A. Duncan, and A. Deino (2004), Geochronology of age-progressive volcanism of the Oregon High Lava Plains: Implications for the plume interpretation of Yellowstone, *J. Geophys. Res.*, *109*, B10202, doi:10.1029/2003JB002776.

Kistler, R. W., and Z. E. Peterson (1978), Reconstruction of crustal blocks of California on the basis of initial strontium isotopic compositions of Mesozoic granitic rocks, *U.S. Geol. Surv. Prof. Pap. 1071*, 17 pp.

Koppers, A. A. P. (2002), ArArCALC—Software for 40Ar/39Ar age calculations, *Comput. Geosci.*, *28*(5), 605–619, doi:10.1016/S0098–3004(01)00095-4.

Kuntz, M. A., H. R. Covington, and L. T. Schorr (1992), An overview of basaltic volcanism of the eastern Snake River Plain, Idaho, in *Regional Geology of Eastern Idaho and Western Wyoming*, edited by P. K. Link, M. A. Kuntz, and L. B. Platt, *Geol. Soc. Am. Memoir*, *179*, 227–267.

Larson, E. E. (1965), The structure, stratigraphy, and paleomagnetics of the Plush area, southeastern Lake County, Oregon, Ph.D. thesis, 166 pp., Univ. of Colo., Boulder, Colo.

Lawrence, R. D. (1976), Strike-slip faulting terminates the Basin and Range province in Oregon, *Geol. Soc. Am. Bull.*, *87*, 846–850, doi:10.1130/0016–7606(1976)87<846:SFTTBA>2.0.CO;2.

Long, M. D., and P. G. Silver (2008), The subduction zone flow field from seismic anisotropy: A global view, *Science*, *319*, 315–318, doi:10.1126/science.1150809.

Long, M. D., H. Gao, A. Klaus, L. S. Wagner, M. J. Fouch, D. E. James, and E. Humphreys (2009), Shear wave splitting and the pattern of mantle flow beneath eastern Oregon, *Earth Planet. Sci. Lett.*, *288*, 359–369, doi:10.1016/j.epsl.2009.09.039.

Long, M. D., C. B. Till, K. A. Druken, R. W. Carlson, L. S. Wagner, M. J. Fouch, D. E. James, T. L. Grove, N. Schmerr, and C. Kincaid (2012), Mantle dynamics beneath the Pacific Northwest and the generation of voluminous back-arc volcanism, *Geochem. Geophys. Geosyst.*, *13*, Q0AN01, doi:10.1029/2012GC004189.

Luedke, R. G., and R. L. Smith (1984), Map showing distribution, composition, and age of late Cenozoic volcanic centers in the western conterminous United States. *U. S. Geol. Surv. Misc. Invest. Ser. Map I-1523*, scale 1:2,500,000.

Maclean, J. W. (1994), Geology and geochemistry of Juniper Ridge, Horsehead Mountain and Burns Butte: Implications for the petrogenesis of silicic magma on the High Lava Plains, southeastern Oregon, M.S. thesis, 141 pp., Oreg. State Univ., Corvallis.

MacLeod, N. S., G. W. Walker, and E. H. McKee (1976), Geothermal significance of eastward increase in age of upper Cenozoic rhyolitic domes in southeastern Oregon, paper presented at Second United Nations Symposium on the Development and Use of Geothermal Resources, vol. 1, pp. 465–474, San Francisco.

MacLeod, N. S., D. R. Sherrod, L. A. Chitwood, and R. A. Jensen (1995), Geologic map of Newberry Volcano, Deschutes, Klamath, and Lake Counties, Oregon, *U.S. Geol. Surv. Misc. Invest. Ser. Map I-2455*, scale 1:62,500 and 1:24,00.

Mathis, A. C. (1993), Geology and petrology of a 26-Ma trachybasalt to peralkaline rhyolite suite exposed at Hart Mountain, Oregon, M.S. thesis, 141 pp., Oreg. State Univ., Corvallis.

McCrory, P. A., J. L. Blair, F. Waldhauser, and D. H. Oppenheimer (2012) Juan de Fuca slab geometry and its relation to Wadati-Benioff zone seismicity, *J. Geophys. Res.*, *117*, B09306, doi:10.1029/2012JB009407.

McCurry, M., and D. W. Rodgers (2009), Mass transfer along the Yellowstone hotspot track I: Petrologic constraints on the volume of mantle-derived magma, *J. Volcanol. Geotherm. Res.*, *188*, 86–98, doi:10.1016/j.jvolgeores.2009.04.001.

McCurry, M., K. P. Hayden, L. H. Morse, and S. Mertzman (2008), Genesis of post-hotspot, A-type rhyolite of the Eastern Snake River Plain volcanic field by extreme fractional crystallization of olivine tholeiite, *Bull. Volcanol.*, *70*, 361–383, doi:10.1007/s00445-007-0143-4.

McKee, E. H., and G. W. Walker (1976), Potassium-argon ages of late Cenozoic silicic volcanic rocks, southeastern Oregon, *Isochron West*, *15*, 37–41.

McQuarrie, N., and D. Rodgers (1998), Subsidence of a volcanic basin by flexure and lower crustal flow: The eastern Snake River Plain, Idaho, *Tectonics*, *17*, 203–220, doi:10.1029/97TC03762.

Meigs, A., et al. (2009), Geological and geophysical perspectives on the magmatic and tectonic development, High Lava Plains and northwest Basin and Range, in *Volcanoes to Vineyards: Geologic Field Trips Through the Dynamic Landscape of the Pacific Northwest*, edited by J. E. O'Connor, R. J. Dorsey, and I. P. Madin, *Geol. Soc. Am. Field Guide, 15*, 435–470.

Miller, R. J., G. L. Raines, and K. A. Connors (2003), Spatial digital database for the geologic map of Oregon, *U. S. Geol. Surv. Open File Rep. 03-67*, 21 pp.

Milliard, J. B. (2010), Two-stage opening of the northwestern Basin and Range in eastern Oregon, M.S. thesis, 81 pp., Oreg. State Univ., Corvallis.

Min, K., R. Mundil, P. R. Renne, and K. R. Ludwig (2000), A test for systematic errors in 40Ar/39Ar geochronology through comparison with U/Pb analysis of a 1.1-Ga rhyolite, *Geochim. Cosmochim. Acta*, *64*, 73–98, doi:10.1016/S0016–7037(99)00204-5.

Naoum, S., and I. K. Tsanis (2004), Ranking spatial interpolation techniques using a GIS-based DSS, *Global Nest Int. J.*, *6*, 1–20.

Nekvasil, H., A. Simon, and D. H. Lindsley (2000), Crystal fractionation and the evolution of intra-plate hy-normative igneous suites: Insights from their feldspars, *J. Petrol.*, *41*, 1743–1757, doi:10.1093/petrology/41.12.1743.

Newton, V. C., R. E. Corcoran, and R. J. Deacon (1962), Oregon, still without oil, offers favorable pay areas, in petroleum exploration in Oregon, *Oreg. Dep. Geol. Miner. Ind. Misc. Pap. 9*, 1–5.

Otto, B. R., and D. A. Hutchison (1977), The geology of Jordan Craters, Malheur County, Oregon, *Ore Bin*, *39*, 125–140.

Pavlis, G. L., K. Sigloch, S. Burdick, M. J. Fouch, and F. Vernon (2012), Unraveling the geometry of the Farallon Plate: Synthesis of three-dimensional imaging results from the USArray, *Tectonophysics*, *532–535*, 82–102, doi:10.1016/j.tecto.2012.02.008.

Pezzopane, S., and R. J. Weldon (1993), Tectonic role of active faulting in central Oregon, *Tectonics*, *12*, 1140–1169, doi:10.1029/92TC02950.

Pierce, K. L., and L. A. Morgan (1992), The track of the Yellowstone hotspot: Volcanism, faulting and uplift, in *Regional Geology of Eastern Idaho and Western Wyoming*, edited by P. K. Link, M. A. Kuntz, and L. B. Platt, *Geol. Soc. Am. Memoir, 179*, 1–53.

Popenoe, H. L. (1961), Developments in west coast area in 1960, *Bull. Am. Assoc. Pet. Geol.*, *45*, 959–973.

Renne, P. R., C. C. Swisher, A. L. Deino, D. B. Karner, T. L. Owens, and D. J. DePaolo (1998), Intercalibration of standards, absolute ages and uncertainties in 40Ar/39Ar dating, *Chem. Geol.*, *145*, 117–152, doi:10.1016/S0009–2541(97)00159-9.

Robinson, P. T., G. W. Walker, and E. H. McKee (1990), Eocene (?), Oligocene, and lower Miocene rocks of the Blue Mountains Region, in *Geology of the Blue Mountains Region of Oregon, Idaho, and Washington*, edited by G. W. Walker, *U.S. Geol. Surv. Prof. Pap. 1437*, 29–62.

Rosenberg, C. L., S. Medvedev, and M. R. Handy (2007), *Effects of melting on faulting and continental deformation, in Tectonic Faults: Agents of Change on a Dynamic Earth, Dahlem Workshop Rep. 95*, edited by M. R. Handy, G. Hirth, and N. Hovius, pp. 357–401, MIT Press, Cambridge, Mass.

Roth, J. B., M. J. Fouch, D. E. James, and R. W. Carlson (2008), Three-dimensional seismic velocity structure of the northwestern United States, *Geophys. Res. Lett.*, *35*, L15304, doi:10.1029/2008GL034669.

Russell, I. C. (1884), A geological reconnaissance in Southern Oregon, *U. S. Geol. Surv. Annu. Rep. 4*, 431–464.

Russell, I. C. (1905), Preliminary report on the geology and water resources of Central Oregon, *U.S. Geol. Surv. Bull.*, *252*, 138 pp.

Russell, J. K., and J. Nicholls (1987), Early crystallization history of alkali olivine basalts, Diamond Craters, Oregon, *Geochim. Cosmochim. Acta*, *51*, 143–154, doi:10.1016/0016–7037(87)90015-9.

Scarberry, K. C. (2007), Extension and volcanism: Tectonic development of the northwestern margin of the Basin and Range Province in southern Oregon, Ph.D. thesis, 168 pp., Oreg. State Univ., Corvallis.

Scarberry, K. C., A. J. Meigs, and A. L. Grunder (2010), Faulting in a propagating continental rift: Insight from the late Miocene structural development of the Abert Rim fault, southern Oregon, *USA, Tectonophysics*, *488*, 71–86, doi:10.1016/j.tecto.2009.09.025.

Schmidt, M. E., and A. L. Grunder (2011), Deep Mafic Roots to Arc Volcanoes: Mafic recharge and differentiation of Basaltic Andesite at north Sister Volcano, Oregon Cascades, *J. Petrol.*, *52*, 603–641, doi:10.1093/petrology/egq094.

Shepard, D., (1968), A two-dimensional interpolation function for irregularly-spaced data, in *Proceed. Assoc. Computing Machinery (ACM) National Conference*, 517–524.

Sherrod, D. R., E. M. Taylor, M. L. Ferns, W. E. Scott, R. M. Conrey, and G. A. Smith (2004), *U.S. Geol. Surv. Geol. Invest. Ser. Map. I-2683*, pamphlet, pp. 1–49.

Sherrod, D. R., D. E. Champion, and J. P. McGeehin (2012), Age and duration of volcanic activity at Diamond Craters, southeastern Oregon, *J. Volcanol. Geotherm. Res.*, *247-248*, 108–114, doi:10.1016/j.jvolgeores.2012.08.008.

Shoemaker, K. A., and W. K. Hart (2002), Temporal controls on basalt genesis and evolution on the Owyhee Plateau, Idaho and Oregon, in *Tectonic and Magmatic Evolution of the Snake River Plain Volcanic Province,* edited by B. Bonnichsen, C. M. White, and M. McCurry, *Idaho Geol. Surv. Bull. 30*, 313–328.

Smith, G. A., L. W. Snee, and E. M. Taylor (1987), Stratigraphic, sedimentologic, and petrologic record of late Miocene subsidence of the central Oregon High Cascades, *Geology*, *15*, 389–392, doi:10.1130/0091–7613(1987)15<389:SSAPRO>2.0.CO;2.

Smith, R. L., and R. G. Luedke (1984), Potentially active volcanic lineaments and loci in western conterminous United States, in, *Explosive Volcanism: Inception, Evolution and Hazards, National Research Council*, pp. 47–66, Natl. Acad. Press, Washington, D. C.

Steiger, R. H., and E. Jager (1977), Subcommission on Geochronology—Convention on the use of decay constants in geochronology and cosmochronology, *Earth Planet. Sci. Lett.*, *36*, 359–363, doi:10.1016/0012–821X(77)90060-7.

Streck, M. (2002), Partial melting to produce high-silica rhyolites of a young bimodal suite: Compositional constraints among rhyolites, basalts, and metamorphic xenoliths from the Harney Basin, Oregon, *Int. J. Earth Sci.*, *91*, 583–593, doi:10.1007/s00531-001-0246-7.

Streck, M. J., and A. L. Grunder (1995), Crystallization and welding variations in a widespread ignimbrite sheet; the Rattlesnake Tuff, eastern Oregon, *USA, Bull. Volcanol.*, *57*, 151–169.

Streck, M. J., and A. L. Grunder (1997), Compositional gradients and gaps in High-silica Rhyolites of the Rattlesnake Tuff, Oregon, *J. Petrol.*, *38*, 133–163, doi:10.1093/petroj/38.1.133.

Streck, M. J., and A. L. Grunder (1999), Enrichment of basalt and mixing of dacite in the rootzone of a large rhyolite chamber: Inclusions and pumices from the Rattlesnake Tuff, Oregon, *Contrib. Mineral. Petrol.*, *136*, 193–212, doi:10.1007/s004100050532.

Streck, M. J., and A. L. Grunder (2008), Phenocryst-poor rhyolites of bimodal, tholeiitic provinces: The Rattlesnake Tuff and implications for mush extraction models, *Bull. Volcanol.*, *70*, 385–401, doi:10.1007/s00445-007-0144-3.

Streck, M. J., and A. L. Grunder (2012), Temporal and crustal effects on differentiation of tholeiite to calcalkaline and ferro-trachytic suites, High Lava Plains, Oregon, *USA, Geochem. Geophys. Geosyst.*, *13*, Q0AN02, doi:10.1029/2012GC004237.

Taylor, E. M. (1981), Central High Cascade roadside geology, in *Guides to Some Volcanic Terranes in Washington Idaho, Oregon, and Northern California*, edited by D. A. Johnston and J. M. Donnelly-Nolan, *U. S. Geol. Surv. Circ*. *838*, 55–83.

Trench, D., A. J. Meigs, and A. L. Grunder (2012), Termination of the northwestern Basin and Range Province into a clockwise rotating region of transtension and volcanism, *J. Struct. Geol.*, *39*, 52–65, doi:10.1016/j.jsg.2012.03.007.

Tucker, K. B., M. J. Iademarco, and A. L. Grunder (2011), The Hampton Tuff, eastern Oregon: Evidence for westward and temporal decline in rhyolitic activity of the High Lava Plains, *Geol. Soc. Am. Abstr. Programs*, *43*(4), 5.

Walker, G. W. (1974), Some implications of Late Cenozoic volcanism to geothermal potential in the High Lava Plains of south-central Oregon, *Ore Bin*, *36*, 109–119.

Walker, G. W., and N. S. MacLeod (1991), Geologic map of Oregon, *U.S. Geol. Surv.*, scale 1:500,000.

Walker, G. W., and P. T. Robinson (1990), Paleocene (?), Eocene and Oligocene (?) rocks of the Blue Mountains region, in *Geology of the Blue Mountains Region of Oregon, Idaho, and Washington*, edited by G. W. Walker, *U. S. Geol. Surv. Prof. Pap. 1437*, 13–27.

Walker, G. W., and D. A. Swanson (1968), Laminar flowage in a Pliocene soda rhyolite ash-flow tuff, Lake and Harney Counties, Oregon, *U. S. Geol. Surv. Prof. Pap. 600-B*, B37–B47.

Watson, D. F., and G. M. Philip (1985), A refinement of inverse distance weighted interpolation, *Geo-Processing*, *2*, 315–327.

Wells, R. E. (1979), Drake Peak—A structurally complex rhyolite center in southeastern Oregon, *U. S. Geol. Surv. Prof. Pap. 1124*, E1–E16.

Williams, H. (1935), Newberry Volcano of central Oregon, *Geol. Soc. Am. Bull.*, *46*, 253–304.

Xue, M., and R. M. Allen (2006), Origin of the Newberry Hotspot Track: Evidence from shear-wave splitting, *Earth Planet. Sci. Lett.*, *244*, 315–322, doi:10.1016/j.epsl.2006.01.066.

Zandt, G., and E. Humphreys (2008), Toroidal mantle flow through the western U.S. slab window, *Geology*, *36*, 295–298, doi:10.1130/G24611A.1.